Designing a resilient and reliable biomass-to-biofuel supply chain under risk pooling and congestion effects and fleet management

H. Soleimanian Khezerlou, Behnam Vahdani, M. Yazdani

Designing a Resilient and Reliable Biomass-to-Biofuel Supply Chain under Risk Pooling and Congestion Effects and Fleet Management

H. Soleimanian Khezerlou[a], Behnam Vahdani[1,a,b], M. Yazdani[a]

[a]*Department of Industrial Engineering, Faculty of Industrial and Mechanical Engineering, Qazvin Branch, Islamic Azad University, Qazvin, Iran*

[b]*IMT Atlantique, Lab-STICC, UBL, F-29238 Brest, France*

Abstract

The utilization of renewable biomass as feedstock for biofuel production has been gaining prestige to mitigate carbon emissions. This paper aims to render an optimization model for designing a resilient and reliable biomass-to-biofuel supply chain network in which multi-modal terminals, biorefineries, and their connection link could be faced with disruption. For this purpose, risk-averse optimization, transitional probabilities, and spatial statistics models are employed. What is more, to overcome the repercussions of uncertain demand and the availability of raw materials, risk pooling and M/M/1 queuing system are considered. Finally, since the proposed model is an NP-hard problem, two meta-heuristic algorithms called improved ray optimization and colliding bodies optimization are employed to solve the proposed model. Computational results reveal that by increasing 20% of the conversion rate of biomass to biofuel, which leads to increase biomass supply, biofuel production increases by 20.88%, and the SC cost declines by 9.32% due to the better capacity distribution of bio-refineries. Also, the proposed model increases by 20.87% in the total SC costs under random disruptions than the risk-neutral model, although the failure costs of SC decline by 80.45%.

Keywords: Biomass supply chain; Disruption; Risk measures; Risk pooling; Congestion; Meta-heuristic

1. Introduction

Nowadays, biofuels production based on cellulosic feedstock has been gaining prestige as sustainable renewable energy (Zahraee et al. 2019). In order to achieve a purpose of producing 16 billion gallons of cellulosic ethanol in 2022, nothing more than 200 million Mg of biomass will be demanded per annum, regarding the ratio of transformation of cellulosic ethanol that is almost equal to 70–90 gallons per Mg of dry cellulosic biomass (Lim et al. 2019). However, there are a limited number of mercantile cellulosic ethanol facilities owing to a lack of reliable resources to supply feedstock for them and economical technology (Jin et al. 2019).

On the one hand, facilities and transportation infrastructure encounter various disruption risks from both natural and human-made disasters. In either circumstance, the supply chain (SC) possibly encounters significant losses (Wang et al. 2020). Hence, in order to mitigate the repercussions of disruptions and losses, creating resilient and reliable SCs is one of the crucial measures. In terms of resiliency, there are two main approaches in the literature, including risk-neutral and risk-averse, such that the risk-averse approach can provide more robustness of solutions than the other, especially under an uncertain condition (Yu et al., 2017). In this regard, a number of risk measurement methods, including value at risk and conditional-value-at-risk, have been applied to incorporate the risk preference. It is worth noting that the second approach can provide a healthy circumstance to quantify the decision-makers' risk preferences and resiliency (Zhu et al. 2020). In terms of reliability, there are four main approaches in the literature, including constant (Salimi and Vahdani, 2018) and variable transitional probabilities (Mohammadi et al. 2020) for assignment decision, scenario-based stochastic programming (Yu et al. 2018) and Monte Carlo simulation (Ngan et al. 2020). The first three approaches are typically applied for a mathematical framework, whereas simulation techniques are usually used when it is impossible to provide a closed-form mathematical model. It is worth noting that the variable

[1] Corresponding author
Email: behnam.vahdani@imt-atlantique.fr

transitional probabilities approach can provide a more reliable general framework in the face of disruptions of facilities (Ulucak, 2020).

On the other hand, there is a broad range of concerns regarding biomass supply planning, including seasonality, widespread and scattered resources, and uncertainty. In this regard, uncertainty in demands due to the competitive business environment significantly influences biofuel SC performance (Ji et al. 2020). One of the efficacious approaches to surmount this challenge is a risk-pooling strategy, which can provide a healthy service level of inventory (Momenikiyai et al. 2018). In addition, due to the availability of raw materials such as harvesting periods of biomass, biorefineries are typically congested. This not only increases SC costs but also decreases the efficiency of biorefineries. From this point of view, a queuing system could be employed to alleviate the repercussions of congestion issues (Poudel et al. 2018).

As far as reliable SC is concerned, Cui et al. (2010) developed variable transitional probabilities for assignment decision to provide a reliable decision for the location-allocation problem under the risk of disruptions. Vahdani et al. (2012) investigated the disruption of collection centers in a closed-loop SC to offer a reliable iron and steel SC. Besides, they utilized an M/M/1 queuing system to estimate the scrap processing facility's capacity. Marufuzzaman et al. (2014) considered the disruptions of two types of facilities, including intermodal hub and biorefinery, to design a reliable three-echelon biofuel SC. Poudel et al. (2016) introduced a spatial statistics model to estimate connection links' reliability, so as to design a reliable biofuel SC, where the disruption links between two types of facilities were considered. This approach can accurately predict the failure probability of connection links when historical data concerning disruptions or disasters might not be attainable. Yildiz et al. (2016) introduced three different methods to compute the cumulative index of reliability for a facility and the facility's arcs input to present a reliable SC. Poudel et al. (2018) extended Marufuzzaman et al. (2014) research by considering an M/M/1 queuing system to tackle the facility congestion due to the feedstock seasonality aspect. Salimi and Vahdani (2018) investigated the disruptions of one type of facility and connection links to render a reliable biofuel SC. In this regard, they utilized the spatial statistics model proposed by (Poudel et al. 2016) to estimate connection links' reliability and risk pooling method to overcome demand uncertainty. Tolooie et al. (2020) considered the disruption of collection centers. They utilized a scenario-based stochastic programming model to provide a reliable SC, where a number of scenarios were also defined to tackle the uncertain demand.

As far as resilient SC is concerned, Gong et al. (2014) presented some restoration strategies to develop a resilient supply chain (RSC) to tackle the challenges of infrastructure disruptions, including supply, communications, and transportation. Also, a two-stage scenario-based solution approach was also proposed to plan restoration measures. Rezapour et al. (2017) investigated the influence of supplier's disruption to render an RSC under competition. They proposed a stochastic model by defining three scenarios, including holding emergency stock, devoting back-up capacity, and multiple-sourcing. Zahiri et al. (2017) considered sustainable and resilient factors in designing an SC under technology disruption at the production facility. To this end, they introduced five factors to consider resiliency, including node critically, flow complexity, node complexity, customer de-service level, and reassignment policy. Fattahi et al. (2017) proposed a multi-stage scenario-based stochastic programming approach to design a responsive and resilient SC to surmount the challenges of facilities' capacities disruptions, in which responsiveness risk and delivery lead-time were considered as two main constraints. To render a resilient scheme for customer assignment in a location-allocation problem, an optimization model was developed by Yu et al. (2017), where the risks were considered by absolute-semi deviation and conditional value-at-risk. What is more, they computed the variable transitional probabilities for assignment decisions based on (Cui et al. 2010). Margolis et al. (2018) introduced an integrated framework to provide a trade-off between entire SC connectivity maximization and total SC cost minimization to design an RSC under facility disruption. Elluru et al. (2019) studied the repercussions of facility disruption and route blockage to offer an RSC by introducing proactive and reactive mechanisms. The proactive method included preventive measures and the reactive one contained re-routing and expanding facility capacity. Pavlov et al. (2019) proposed a new framework to optimize the network

redundancy and contingency planning under facility and supply disruptions, so as to design a resilient and sustainable SC based on the synchronization of structure and flow-oriented approach. Hasani (2021) presented a multi-objective scenario-based stochastic programming model under facility disruption to design a green and resilient SC. In addition, a robust optimization approach was employed to tackle the uncertainty of demands and various costs. As a final point, in an attempt to illustrate the research gap, a comparative table of the investigated studies on resilient and reliable SC network design is presented in Table 1.

Table 1. A comparative literature review on resilient and reliable supply chain network design

Authors and Year	Features	Transitional probabilities for assignment decision		Probability of link failure		Risk pooling	Congestion	Risk measure	Solution approach		
		Parameter	Variable & Level assignment	Constant parameter	Spatial statistics				Commercial solver[1]	Exact[2]	Heuristic/ Meta-heuristic
Vahdani et al. (2012)	Reliable	✓							✓		
Marufuzzaman et al. (2014)	Reliable	✓								✓	
Gong et al. (2014)	Resilient & Restorative	✓		✓					✓		
Poudel et al. (2016)	Reliable				✓					✓	
Yildiz et al. (2016)	Reliable	✓		✓							✓
Rezapour et al. (2017)	Resilient & Competitive	✓							✓		
Fattahi et al. (2017)	Resilient & Responsive	✓									
Zahiri et al. (2017)	Resilient & Sustainable	✓									✓
Poudel et al. (2018)	Reliable	✓					✓				✓
Salimi and Vahdani (2018)	Reliable	✓			✓	✓					✓
Margolis et al. (2018)	Resilient	✓									✓
Elluru et al. (2019)	Resilient	✓							✓		
Pavlov et al. (2019)	Resilient & Sustainable	✓									✓
Tolooie et al. (2020)	Reliable	✓									✓
Hasani (2021)	Resilient & Green	✓									✓
Current research	Reliable & Resilient	✓	✓		✓	✓	✓	✓	✓		✓

1.Lingo, GAMS, CPLEX and AMPL
2.Benders decomposition, Lagrangian relaxation and column generation

As can be seen, researchers have conducted several studies related to the presentation of a resilient or reliable supply chain, in which other considerations such as sustainability, responsiveness, green, restoration, and competition have been reflected. However, considerations of both resiliency and reliability have not been considered. Additionally, two practical approaches related to reliability and resiliency, including variable transitional probabilities for assignment decision and conditional value-at-risk, have not been used to overcome the concerns of facility disruption and risk preference in supply chain network design. What is more, so as to consider the reliability and resiliency in the literature, one of the following three assumptions has been considered: 1) failure of one type of facility, 2) failure of two types of facilities, and 3) failure of one type of facility and its connection path to another facility, while it is clear that the possibility of failure of both facilities and their connection path is much more likely, which has not been investigated so far. Furthermore, considerations of probabilistic demand for products to control inventory level and availability of raw materials to overcome the congestion challenge in biorefineries have not been considered simultaneously. It should be noted that changes in demand can lead to alterations in transportation fleet planning, so fleet management is probably a vital requirement. However, this issue has not been addressed in the context of demand uncertainty.

Hence, in this paper, a mathematical model is proposed to design a resilient and reliable biomass-to-biofuel SC, in which multi-modal terminal and biorefineries as the two major facilities and the connecting link between them could be disrupted. To overcome the concerns of facility and connection link disruptions, two practical approaches, including the variable transitional probabilities method and the spatial statistics model, are employed, respectively. In this regard, in order to consider risk preference as the factor of resiliency, the conditional value-at-risk approach is applied. What is more, the risk-pooling and the congestion effects on facilities are considered to take advantage of inventory systems, cost savings, and to overcome demand uncertainty and seasonality effects of raw material. Also, since the proposed model is an NP-hard problem, two new meta-heuristic algorithms called improved ray optimization and colliding bodies optimization are employed to solve the proposed model.

This paper's remnant is structured as follows: A framework of the proposed model is provided in Section 2. The proposed solution approaches are explained in Section 3. Numerical results and sensitivity analysis, and management insights are provided in Section 4. Lastly, the paper is concluded in Section 5.

2. Problem definition and formulation

A multi-echelon biomass-biofuel SC is considered in this paper, including different feedstock resources, chipping terminals, multi-modal terminals, biorefineries, and customers. The primary feedstock resources include corn-stover, forest residues, and municipal solid waste (MSW). In this regard, the former one is typically available from September to November; the latter one is typically unavailable from December to February, and the third one is usually available all year round. It should be pointed out corn-stover provides in bale format, so it requires no additional decreasing scale in chipping terminals. Also, corn-stover can be transported directly to biorefineries if the chipping terminal is located near to biorefineries (Quddus et al. 2018). Since, in practice, facilities and transportation infrastructure encounter various disruption risks from both natural and human-made disasters, the possibility of disruption is considered for multi-modal terminals, biorefineries, and connection links among them. It should be noted that the failure probabilities of these facilities and connection links are independent. In an attempt to estimate the probability of link failure with respect to the disaster disruption data, a spatial statistics model is applied. This model can identify a subset of connection links, which requires to be strengthened to enhance post-disaster connectivity under a limited amount of budget and can provide an accurate prediction of failure probability of connection links when historical data concerning disruptions or disasters might not be attainable. Moreover, in terms of reflecting the disruption of facilities in an optimization model, two approaches are considered. They include constant and variable transitional probabilities for assignment decisions. Such that the first one is considered for the disruption of multi-modal terminals, and the second one is considered for the disruption of biorefineries.

Additionally, in an attempt to compute resilient location and assignment solutions, two efficient risk measurement methods, including absolute-semi deviation (ASD) and conditional value at risk (CVaR), are applied to incorporate the risk preference of decision-makers (DMs). These approaches can provide a more reliable general framework in the face of disruptions of facilities. Furthermore, in an attempt to mitigate the repercussions of fluctuating demand, a risk-pooling strategy has been applied as one of the rewarding approaches to manipulate such demand uncertainty. Regarding the seasonal aspect of feedstocks, the impact of congestion is reflected in this study by an $M/M/1$ queuing system. The aim of this study is to minimize the expected total cost under the considerations mentioned above. In this regard, a broad range of decisions, including the amount of shipping biomass, the number of required vehicles, location, allocation and capacities of facilities, customer assignment probability, and the reliability improvement achieves by fortifying connection links, are determined. Also, Fig. 1 renders a guideline for better demonstrating the relationships among the whole, decision, and mathematical perspectives, and Fig.2 depicts a graphic demonstration of the investigated problem. It should be pointed out corresponding sets, indices, parameters, and decision variables to formulate the problem can be found in the nomenclature. The main assumptions of the current research are as follows:

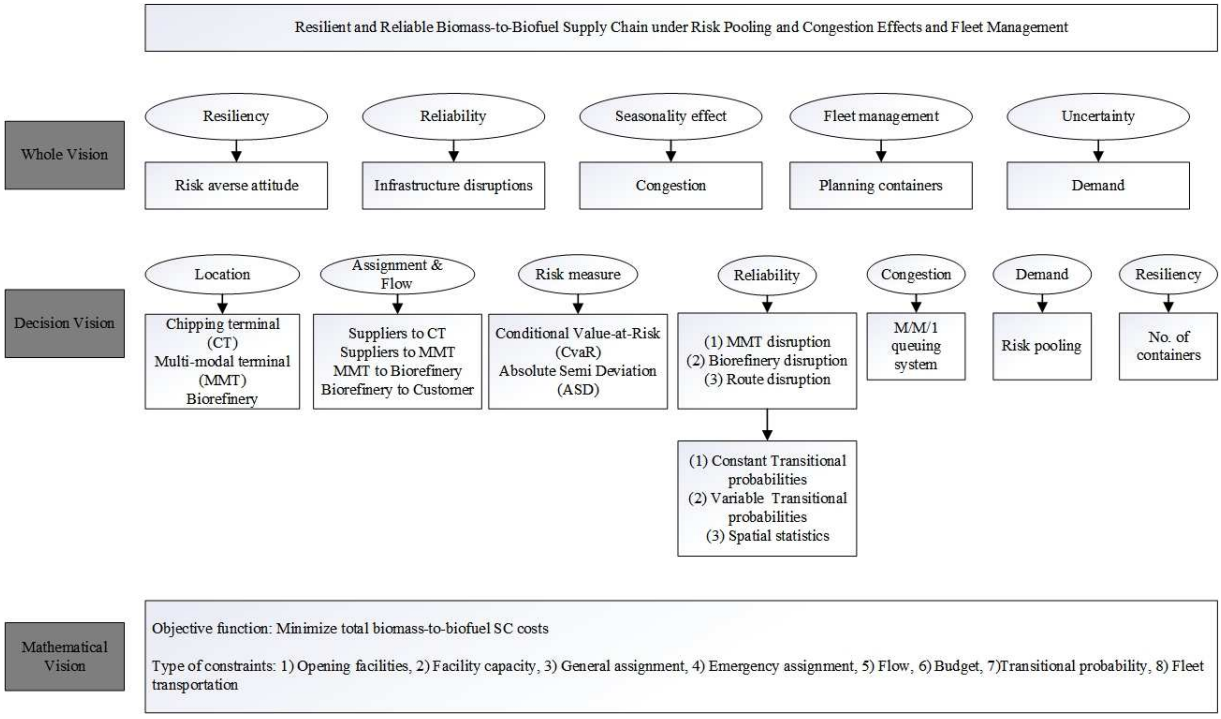

Fig1. A guideline for demonstrating different levels of planning

- The demand of customers is normally distributed with specified mean and variance.
- Each biorefinery follows a continuous review policy (Q, r) with a service level constraint.
- Disruptions of multi-modal terminals and biorefineries are mutually independent.
- Disruptions of facilities and connection links are mutually independent.
- The DM holds a predefined preference over the planning horizon.
- There are no other rivals in each region.

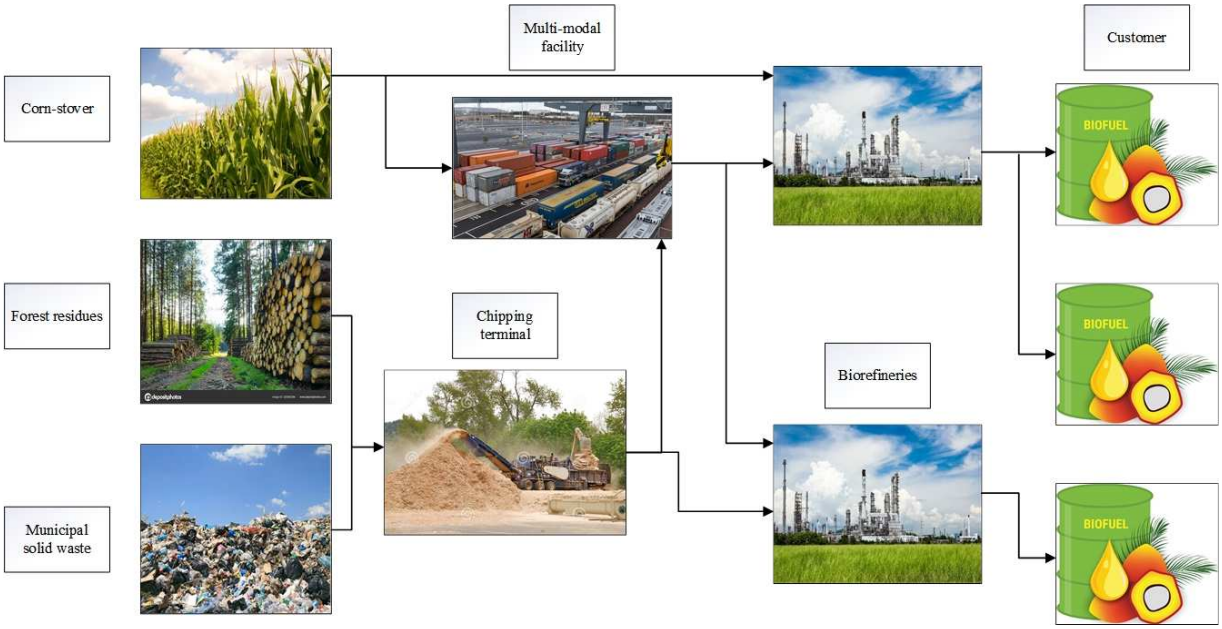

Fig.2. The graphic demonstration of the investigated problem

2.1. Spatial statistics *model of link failure probability*

Assume that connection link (j,k) can be compartmented into n_{jk} segments, each of them has a failure probability of q_ℓ for $\ell = 1,2,\dots,n_{jk}$, so q_{jk} can be estimated as $q_{jk} = \max_{\ell=1,2,\dots,n_{jk}} q_\ell$, and the continuous spatial statistics model is as follows (Poudel et al., 2018):

$$q(s) = \mu + e(s) \tag{1}$$

where s signifies long-latitude synchronizes for the potential location of biomass configuration, μ signifies the average probability of disaster event and $e(s)$ signifies spatial process with predefined mean and a covariance configuration, so semi-variogram function $\gamma(h)$ is as follows:

$$\gamma(h) = \frac{1}{2}\mathrm{Var}[q(s) - q(s+h)] \tag{2}$$

Given the perceived historical data of failure probability, i.e., $q(s_1),\dots,q(s_n)$, the empirical estimation of $\gamma(h)$ is as follows (Poudel et al., 2018):

$$\hat{\gamma}(h) = \frac{1}{2|N(h)|}\sum_{N(h)}\{q(s_i) - q(s_j)\}^2 \tag{3}$$

where $N(h)$ signifies the set of location pair (s_i, s_j) with a synchronize difference h, an $|N(h)|$ signifies the number of dissimilar pairs. In what follows, let $q = (q(s_1),\dots,q(s_n))'$ as the set of existing historical data of failure probability. The Ordinary Kriging predictor for a location s_0 is a linear estimator in the form of $\hat{q}_{0k}(s_0) = \lambda' q$, where λ signifies the unknown coefficients of weight to be estimated. For this purpose, define $\lambda = (\lambda_1,\dots,\lambda_n)'$ as follows (Poudel et al., 2018):

$$\text{Min } L = E\left[\left(\lambda' q(s) - q(s_0)\right)^2\right]$$

S.t.:

$$\sum_{i=1}^{n} \lambda_i = 1. \tag{4}$$

This problem can be solved by utilizing the Lagrangian method as follows:

$$\arg min_{\lambda,\theta} L = argmin_{\lambda,\theta}\left\{E\left[\left(\lambda' q - q(s_0)\right)^2\right] - 2\theta\left(\sum_{i=1}^{n} \lambda_i - 1\right)\right\} \tag{5}$$

Let $\Gamma = \left[\gamma\left(s_i - s_j\right)\right]$ and $\gamma(s_0) = [\gamma(s_0 - s_1), \dots, \gamma(s_0 - s_n)]'$as a semi-variogram matrix of available data and semi-variogram vector between s_0 and $\{s_1, \dots, s_n\}$. The obtained estimation by Ordinary Kriging is as follows (Poudel et al., 2018):

$$\hat{q}_{0k}(s_0) = \lambda' q(s) \tag{6}$$

where

$$\lambda' = \left(\gamma(s_0) + \mathbf{1}\frac{1 - \mathbf{1}'\Gamma^{-1}\gamma(s_0)}{\mathbf{1}'\Gamma^{-1}\mathbf{1}}\right)' \Gamma^{-1} \tag{7}$$

2.2. Risk pooling

In this paper, a continuous review policy (Q, r) is employed in order to manage the service level of inventory in biorefineries. This policy presumes that a replenishment order with the constant quantity (Q) is issued on each moment the level of inventory is at or underneath the constant reorder point (r). Assume that the demand of each customer $g \in G$ is $N\sim(\mu_g, \sigma_g^2)$, and $\sigma_g^2/\mu_g = \zeta, \forall g \in G$, for a constant $\zeta \geq 0$ (Daskin et al., 2002). As in Snyder and Shen, (2011), if there were no disruptions, the optimal expected inventory cost at biorefinery k is calculated by Eq. (8):

$$\mathbb{E}_k = \left(\sqrt{2\theta h_k f_k} + \theta h_k z_\alpha \sqrt{l_k \zeta}\right)\sqrt{\sum_g \mu_g} \tag{8}$$

As regards in Zhang et al., (2016), the approximation of expected inventory cost under disruption is calculated as follows:

$$\mathbb{E}' = \sum_{k\in K} \mathbb{E}_k \sqrt{\sum_{r=0}^{R-1}\sum_{g\in G} \mu_g p_{gkr} z_{gkr}} = \sum_{k\in K} \sqrt{\sum_{g\in G}\sum_{r=0}^{R-1} \widehat{\mathbb{E}}_{gk} p_{gkr} z_{gkr}} \tag{9}$$

where $\widehat{\mathbb{E}}_{gk} = \mu_g \mathbb{E}_k^2$.

This approximation's quiddity propels the expectation for entire the failure states to the square-root term's interior.

2.3. Congestion effect

In the course of peak harvesting periods of biomass, biorefineries are congested, and this phenomenon leads to increase dramatically the costs of the supply chain. The repercussions of congestion on total supply chain costs and the performance of biorefineries become more intensive once the total feedstock flow approaches the capacity of a biorefinery, which can be modeled as an M/M/1 queuing system. An M/M/1 model expresses the queue length in a system with a single server, unrestricted capacity, and unrestricted customer population, where arrivals and service times are ascertained by a Poisson process and an exponential distribution, respectively. So, the system-wide average waiting time subject to steady-state circumstances can be characterized as $\left(\mathcal{U}_k/(\mathcal{C}_k - \mathcal{U}_k)\right)$ for the whole network, where $\mathcal{U}_k$ and $\mathcal{C}_k$ are the total input flow to and the capacity of biorefinery k, respectively, such that once the amount of input feedstock at a biorefinery increases, this proportion will increase exponentially (Poudel et al., 2016). Hence, the congestion cost of the investigated system is calculated as follows:

$$\sum_{k\in K} \mathcal{C}_0 \left(\frac{\sum_{i\in I_c} x_{f_1 ik} + \sum_{f\in F\setminus\{f_1\}} \sum_{s\in S} x_{fsk} + \sum_{f\in F\setminus\{f_1\}} \sum_{s\in S} \sum_{j\in J} x_{fsjk} + \sum_{i\in I_c} \sum_{j\in J} x_{f_1 ijk}}{\sum_{l\in \mathfrak{L}} ca_{lk} y_{lk} - \left(\sum_{i\in I_c} x_{f_1 ik} + \sum_{f\in F\setminus\{f_1\}} \sum_{s\in S} x_{fsk} + \sum_{f\in F\setminus\{f_1\}} \sum_{s\in S} \sum_{j\in J} x_{fsjk} + \sum_{i\in I_c} \sum_{j\in J} x_{f_1 ijk} \right)} \right) \tag{10}$$

Since this congestion term is a nonlinear term, a linearization technique, which was proposed by Elhedhli and Wu (2010), is utilized to linearize it. See **Appendix A** for the explanation about equivalent linearization form.

2.4. Resilient strategy and risk measures

Generally speaking, there are two main kinds of decision-making approaches in cost-effective optimization, including the return-risk trade-off analysis and utility maximization. In the first one, the risk is particularity computed via a risk measure that illustrates loss with a real number. Since this approach can comfort the realization of risk, it has been comprehensively employed in theoretical and practical studies. Whereas the second one demonstrates some theoretical gravity, it explains the risk indirectly. The mean-variance analysis was proposed by Markowitz (1952) as a modern portfolio theory in the context of return-risk trade-off analysis in which variance is reflected as the risk measure. In this regard, another measure of downside risk called Value-at-Risk (VaR) has gained prestige in financial risk management since the middle of the 1990s. Nevertheless, this approach has been impeached regarding three perspectives. Firstly, it is not subadditive in the expected distribution, so it is not a comprehensible risk measure from Artzner et al. (1999). It may also not be comfortable in terms of optimization due to bearing several local extrema for discrete distributions. Finally, it is only a percentile of the loss distribution, so it cannot articulate the extreme nature losses surpassing it. The CvaR was introduced as the mean of the tail distribution surpassing VaR, which has been employed in various fields in recent years. This method offers a number of better features than VaR as a risk measure. Firstly, minimizing CVaR can be attained without predesignating the equivalent VaR by minimizing a more flexible auxiliary function, and in parallel, VaR can be computed as a spin-off (Rockafellar and Uryasev, 2000, 2002). In addition, the formulation of CVaR minimization rendered by Rockafellar and Uryasev (2000, 2002) typically leads to convex and even linear programs. In this regard, another risk measure called absolute semi deviation (ASD) was also proposed to illustrate the entire extent of risk-averse preferences, which the mean-risk method is unable to render it (Zhu and Fukushima, 2009). Therefore, CVaR and ASD are considered as coherent risk measure approaches in order to compute resilient location and customer assignment solutions and incorporate the risk preference of DMs. The CVaR method is formulated as follows:

$$\mathrm{CVaR}_\alpha(Z) = E\{Z | Z \geq \mathrm{VaR}_\alpha(Z)\} \tag{11}$$

Generally speaking, the conservatism degree of DM is denoted by $\alpha \in (0,1)$. Indeed, once $\alpha \to 1$, the measure concentrates on more extreme losses.

Proposition 1. (Rockafellar and Uryasev, 2000). Assume Z has support contained in $[0, \eta_{max}]$, so

$$\mathrm{CVaR}_{\alpha}(Z) = \inf_{\eta \in [0,\eta_{max}]} \{\eta + (1-\alpha)^{-1} E[(Z-\eta)_+]\} \tag{12}$$

where $(Z-\eta)_+ = \max\{Z-\eta, 0\}$.

Proposition 2. (Kusuoka demonstration (Shapiro, 2013)). Absolute-semi deviation is calculated as follows:

$$\mathrm{ASD}(Z) = \{E[\bar{Z} - Z]\Pr(Z)\} = \left\{\int_{-\infty}^{\bar{Z}} (\bar{Z} - \xi)\Pr(Z)(d\xi)\right\} \tag{13}$$

where $\bar{Z} = E(Z) = \int_{-\infty}^{+\infty} \xi \Pr(Z)(d\xi)$, which has a Kusuoka demonstration as follows:

$$\mathrm{ASD}(Z) = E(Z) + \lambda E\{[Z - E(Z)]_+\} = \inf_{t \in \mathbb{R}} \sup_{\kappa \in [0,1]} E[Z + \lambda\kappa(t - Z) + \lambda[Z-t]_+], \tag{14}$$

where the degree of DM's risk-averse attitude is denoted by the constant $\lambda \in [0,1]$.

As mentioned before, the investigated biomass-to-biofuel SC consists of a set of customers G, indexed by g, and a set of candidate biorefinery locations K, indexed by k. The unit transportation cost of biofuel demand from biorefinery k to customer g is given by c_{kg}. Each created biorefinery k is encountered to disruption with probability $0 \le q_k < 1$. In this research, it is assumed q_k in identified a priori. It is assumed that each customer is allocated to up to $R \ge 1$ biorefineries. When a biorefinery fails, the related customer g can be served by a biorefinery at level r $(r \le R-1)$ once biorefineries at level $0,1,\dots,r-1$ have completely failed (Snyder and Daskin, 2005), so R is denoted as the number of back-up biorefineries for a customer. Related with each customer g is a cost π_g that signifies the compensation cost of unfulfilled demand. In order to model this, a dummy biorefinery e that has fixed cost $w_e = 0$, failure probability $q_e = 0$, and unit transportation cost $c_{eg} = \pi_g$ for all customers $g \in G$ is defined (Yu et al., 2017). Let $k_e = k \cup \{e\}$. Therefore, the assignment probability variables can be calculated as follows:

$$p_{gkr} = (1 - q_k) \sum_{n=1}^{K-1} \frac{q_n}{1 - q_n} \, p_{gn(r-1)} z_{gn(r-1)} \tag{15}$$

where Eq. (15) demonstrates the transitional connection between biorefinery n and biorefinery k from level r to level $r-1$ with failure probability q_n. Since $r \in [1, R]$, Eq. (15) can be written as Eq. (16) (Yu et al., 2017):

$$p_{gkr} = (1 - q_k) \frac{q_n}{1 - q_n} \, p_{gk(r-1)} \tag{16}$$

Given that customer g is served by biorefinery n at level $r-1$, so for the classic risk-neutral model, the aim is to minimize the expected costs. It should be noted that the considered unit transportation cost emergency is τ times much as much as c_{fsjk}, where the risk coefficient $\tau \ge 1$ and $\tau = 1$ signifies the risk-neutral case.

$$
\begin{aligned}
\min \mathbb{z} = & \sum_{l\in L}\sum_{s\in S} w_{ls}y_{ls} + \sum_{l\in L}\sum_{j\in J} w_{lj}y_{lj} + \sum_{l\in L}\sum_{k\in K} w_{lk}y_{lk} + \sum_{f\in F\setminus\{f_1\}}\sum_{i\in I\setminus\{I_C\}}\sum_{s\in S}\left(c_{fis}+p_{fi}\right)x_{fis} \\
& + \sum_{i\in I_c}\sum_{k\in K}\left(c_{f_1ik}+p_{f_1i}\right)x_{f_1ik} + \sum_{f\in F\setminus\{f_1\}}\sum_{s\in S}\sum_{k\in K}\left(c_{fsk}+e_{fs}\right)x_{fsk} + \sum_{j\in J}\sum_{k\in K} u_{jk}z_{jk} + \sum_{l\in \mathrm{L}}\sum_{k\in K} cp_{lk}p_{lk} \\
& + \sum_{k\in K}\sqrt{\sum_{g\in G}\sum_{r=0}^{R-1}\widehat{\mathbb{E}}_{gk}p_{gkr}z_{gkr}} + \sum_{k\in K}\mathcal{C}_0V_k \\
& + \sum_{f\in F\setminus\{f_1\}}\sum_{s\in S}\sum_{j\in J}\sum_{k\in K} c_{fsjk}(1-q_j)(1-q_k)\left(1-\left(q_{jk}-\Delta_{jk}\right)\right)x_{fsjk} \\
& + \sum_{f\in F\setminus\{f_1\}}\sum_{s\in S}\sum_{k\in K} c_{fsk}\Bigg[\tau\sum_{j}\left[q_j+q_k+(q_{jk}-\Delta_{jk})-\left[q_jq_k+q_j(q_{jk}-\Delta_{jk})+q_k(q_{jk}-\Delta_{jk})\right]\right. \\
& \left. + q_jq_k(q_{jk}-\Delta_{jk})\right]x_{fsjk}\Bigg] + \sum_{i\in I_c}\sum_{j\in J}\sum_{k\in K}\left(c_{f_1ijk}+p_{f_1i}\right)(1-q_j)(1-q_k)\left(1-\left(q_{jk}-\Delta_{jk}\right)\right)x_{f_1ijk} \\
& + \sum_{i\in I_c}\sum_{k\in K} c_{f_1ik}\Bigg[\tau\sum_{j}\left[q_j+q_k+(q_{jk}-\Delta_{jk})-\left[q_jq_k+q_j(q_{jk}-\Delta_{jk})+q_k(q_{jk}-\Delta_{jk})\right]\right. \\
& \left. + q_jq_k(q_{jk}-\Delta_{jk})\right]x_{f_1ijk}\Bigg] + \sum_{g\in G}\sum_{k\in K}\sum_{r=0}^{R} p_{gkr}z_{gkr}\mu_g\beta c_{kg}
\end{aligned}
\tag{17}
$$

The objective function (17) minimizes the total biomass-to-biofuel SC costs. The first to third terms calculate the opening costs of chipping terminals, multi-modals, and biorefineries, respectively. The fourth term calculates the transportation and procurement costs of biomass from forest residues and MSW suppliers to chipping terminals. The fifth term calculates the transportation and procurement costs of biomass from corn-stover suppliers to biorefineries. The sixth term calculates the chipping costs and transportation costs between chipping terminals and biorefineries. The seventh term computes the fixed costs of utilized containers. The eighth term calculates the production costs in biorefineries, and the ninth one computes the expected inventory cost under disruption in biorefineries. The tenth term calculates the congestion costs in biorefineries. The eleventh term calculates the regular transportation costs for forest residues and MSW biomasses, when multi-modal terminals, biorefineries and connection links between them are available. The twelfth term represents the transportation cost under disruption scenarios. The thirteenth term calculates the regular transportation costs for corn-stover biomass, when multi-modal terminals, biorefineries and connection links between them are available. The fourteenth term represents the transportation cost under disruption scenarios. The fifteenth term calculates the total expected uncertain costs.

2.4.1. CVaR-based risk-averse model

Concerning the description of CVaR and objective function (17), the CVaR-based risk-averse model is represented as Eqs. (18)-(20). It should be noted that network constraints (Subsection 2.5) are added to complete this model. See **Appendix B** for the explanation about obtaining the subsequent model.

$$
\min_{(X,Y,Z,P,\Delta)\in Z}\left\{\mathcal{R}+\sum_{g\in G}\varphi_g(P,Z)\right\}
\tag{18}
$$

S.t.:

$$\mathcal{M}_{gkr} \geq z_{gkr}\mu_g \beta c_{kg} - \eta_g \quad \forall g,k,r \tag{19}$$

$$\mathcal{M}_{gkr} \geq 0 \ \ \forall g,k,r \tag{20}$$

where $\mathcal{R}$ is the remnant of the objective function (17). Indeed Eq. (18) is the total costs of the biomass SC and the risk values for whole customers.

2.4.2. ASD-based risk-averse model

Concerning the description of ASD and objective function (17), the ASD-based risk-averse model is represented as Eqs. (21)-(23). It should be noted that Eqs (19) and (20) and network constraints (Subsection 2.5) are added to complete this model. See **Appendix C** for the explanation about obtaining the subsequent model.

$$\min_{(X,Y,Z,P,\Delta)\in Z,\mathcal{M},\eta,\mathcal{F}} \left\{ \mathcal{R} + \sum_{g\in G} \mathcal{F}_g \right\} \tag{25}$$

S.t.:

$$\mathcal{F}_g \geq \sum_{k\in K}\sum_{r=0}^{R} p_{gkr}\left[z_{gkr}\mu_g \beta c_{kg} + \lambda \mathcal{M}_{gkr}\right] \ \forall g \in G \tag{26}$$

$$\mathcal{F}_g \geq \sum_{k\in K}\sum_{r=0}^{R} p_{gkr}\left[z_{gkr}\mu_g \beta c_{kg} + \lambda\left(\eta_g - z_{gkr}\mu_g \beta c_{kg}\right) + \lambda \mathcal{M}_{gkr}\right] \ \forall g \in G \tag{27}$$

where $\mathcal{R}$ is the remnant of the objective function (21). Indeed Eq. (25) is the total costs of the biomass SC and the risk values for whole customers.

2.5. Network constraints

In this section, the other required constraints are provided to complete optimization model of investigated problem.

$$\sum_{k\in K} x_{f_1 ik} + \sum_{k\in K}\sum_{j\in J} x_{f_1 ijk} \leq s_{f_1 i} \quad \forall i \in I_c \tag{28}$$

$$\sum_{s\in S} x_{fis} \leq s_{fi} \quad \forall f \in F \setminus \{f_1\}, \forall i \in I_w \cup I_m \tag{29}$$

Constraint (28) represents the amount of biomass transported from corn-stover suppliers are restricted by its availability. Constraint (29) represents the amount of biomass transported from forest residues and MSW suppliers are restricted by its availability.

$$\sum_{i\in I_w \cup I_m} r_f x_{fis} = \sum_{k\in K} x_{fsk} + \sum_{j\in J}\sum_{k\in K} x_{fsjk} \quad \forall f \in F \setminus \{f_1\}, \forall s \in S \tag{30}$$

$$\sum_{i\in I_c}\varphi_f\, x_{f_1ik}+\sum_{f\in F\setminus\{f_1\}}\sum_{s\in S}\varphi_f\, x_{fsk}+\sum_{f\in F\setminus\{f_1\}}\sum_{s\in S}\sum_{j\in J}\varphi_f x_{fsjk}+\sum_{i\in I_c}\sum_{j\in J}\varphi_f x_{f_1ijk}=\sum_{l\in L}p_{lk}\quad \forall k\in K \tag{31}$$

$$\sum_{l\in L}p_{lk}\geq\sum_{g\in G}\sum_{r\in R}\mu_g p_{gkr}z_{gkr}\qquad \forall k\in K \tag{32}$$

Constraints (30) and (38) denote the flow balance between facilities. Constraint (31) represents the expected amount of biofuel distributed to the customers is restricted by the amount of biofuel produced in biorefineries. Constraint (32) ensures that the total amount of forest residues and MSW biomasses transported to chipping terminals is restricted by chipping capacity.

$$\sum_{f\in F\setminus\{f_1\}}\sum_{i\in I_w\cup I_m}x_{fis}\leq\sum_{l\in L}ca_{ls}y_{ls}\quad \forall s\in S \tag{33}$$

$$\sum_{i\in I_c}\sum_{k\in K}x_{f_1ijk}+\sum_{f\in F\setminus\{f_1\}}\sum_{s\in S}\sum_{k\in K}x_{fsjk}\leq\sum_{l\in L}ca_{lj}y_{lj} \tag{34}$$

$$\sum_{i\in I_c}x_{f_1ik}+\sum_{f\in F\setminus\{f_1\}}\sum_{s\in S}x_{fsk}+\sum_{i\in I_c}\sum_{j\in J}x_{f_1ijk}+\sum_{f\in F\setminus\{f_1\}}\sum_{s\in S}\sum_{j\in J}x_{fsjk}\leq\sum_{l\in L}ca_{lk}y_{lk}\qquad \forall k\in K \tag{35}$$

$$\sum_{i\in I_c}x_{f_1ijk}+\sum_{f\in F\setminus\{f_1\}}\sum_{s\in S}x_{fsjk}\leq cap_{jk}z_{jk}\quad \forall j\in J,\forall k\in K \tag{36}$$

Constraints (33) to (35) ensure that these facilities have been opened by the time they could provide related service. Besides, constraint (34) ensures that the total amount of biomass transported to multi-modal terminals is restricted by multi-modal terminal capacity. Constraint (35) ensures the total amount of biomass transported to biorefineries is restricted by biorefinery capacity. Constraint (36) ensures the amount of biomass transported to biorefineries cannot transgress the capacity of containers.

$$\sum_{l\in L}y_{ls}\leq 1\qquad \forall s\in S \tag{37}$$

$$\sum_{l\in L}y_{lj}\leq 1\qquad \forall j\in J \tag{38}$$

$$\sum_{l\in L}y_{lk}\leq 1\qquad \forall k\in K \tag{39}$$

$$p_{lk}\leq pca_{lk}y_{lk}\qquad \forall l\in L,\forall k\in K \tag{40}$$

Constraints (37) to (39) ensure that, at most, one capacity level of chipping terminal, multi-modal terminal and biorefinery can be selected. Constraint (40) restricts the capacity of biofuel production in biorefineries and ensures that a biorefinery has been opened by the time it could produce biofuel.

$$\sum_{j\in J}\sum_{k\in K}r_{jk}\Delta_{jk}\leq B \tag{41}$$

$$\Delta_{jk} \leq \bar{\Delta}_{jk} \qquad \forall j \in J, \forall k \in K \tag{42}$$

$$z_{jk} \leq \sum_{l \in L} \min\left\{\left[\frac{ca_{lj}}{cap_{jk}}\right], \left[\frac{ca_{lk}}{cap_{jk}}\right]\right\} y_{lj} \cdot y_{lk} \qquad \forall j \in J, \forall k \in K \tag{43}$$

Constraint (41) restricts the total budget of fortification. Constraint (42) restricts the amount of reliability improvement on connection links. Constraint (43) restricts the maximum number of containers that can be shipped through an active connection link and ensures that multi-modal terminal and biorefinery have been opened by the time this connection could provide related service.

$$p_{gk0} = 1 - q_k \qquad \forall g \in G, \forall k \in K \tag{44}$$

$$p_{gkr} = (1 - q_k) \sum_{n=1}^{K-1} \frac{q_n}{1 - q_n} p_{gn(r-1)} z_{gn(r-1)} \quad \forall g \in G, \forall k \in K, \forall\, 1 \leq r \leq R \tag{45}$$

$$\sum_{k \in K} z_{gkr} + \sum_{a=0}^{r} z_{gea} = 1 \qquad \forall g \in G, 0 \leq r \leq R \tag{46}$$

$$z_{gkr} \leq \sum_{l \in L} y_{lk} \qquad \forall g \in G, \forall k \in K, 0 \leq r \leq R-1 \tag{47}$$

The equations of transitional probability are provided by constraints (44) to (45). Constraint (46) ensures that for each customer g and each level r, either customer g is allocated to an ordinary biorefinery at level r or it is allocated to the dummy biorefinery e at some levels $a \leq r$. Constraint (47) guarantees that customers are only allocated to open biorefineries.

$$\sum_{r=0}^{R-1} z_{gkr} \leq 1 \qquad \forall g \in G, \forall k \in K \tag{48}$$

$$\sum_{r=0}^{R} z_{ger} = 1 \qquad \forall g \in G \tag{49}$$

$$p_{gkr} \in [0,1], x_{fis}, x_{f_1 ik}, x_{fsk}, x_{fsjk}, x_{f_1 ijk}, z_{jk}, p_{lk}, \Delta_{jk} \geq 0, y_{ls}, y_{lj}, y_{lk}, z_{gkr} \in \{0,1\} \tag{50}$$

Constraint (48) ensures that each customer g is not allocated to a given biorefinery k at more than one level. Constraint (49) ensures that each customer to be allocated to the dummy biorefinery at some level, to obtain the opportunity that the whole open biorefineries fail and the customer encounters the cost of lost sales. Constraint (50) denotes the types of decision variables. Additionally, so as to linearize constraint (43), there is

$$y_{lj} \cdot y_{lk} = \mathcal{Y}_{lkj}$$

Moreover, a set of constraints (51) will be eked to other constraints

$$\begin{aligned} &\mathcal{Y}_{lkj} \leq y_{lj} \quad \forall l,k,j \\ &\mathcal{Y}_{lkj} \leq y_{lk} \quad \forall l,k,j \\ &\mathcal{Y}_{lkj} \geq y_{lj} + y_{lk} - 1 \quad \forall l,k,j \end{aligned} \tag{51}$$

3. Solution approaches

Owing to the fact that the proposed optimization model is an NP-hard problem, two new meta-heuristic algorithms called improved ray optimization and colliding bodies optimization are employed to solve the proposed model. The first one was proposed by Kaveh et al., (2013) and the second one was proposed by Kaveh and Mahdavi (2014).

3.1. Improved Ray Optimization (IRO) Algorithm

RO is a population-based meta-heuristic algorithm attributed to the refraction of Snell's light law, once light moves from a lighter to a darker medium, which as proposed by Kaveh and Khayatazad (2012). The improved version of this algorithm was proposed by Kaveh et al., (2013), in which a new approach to overcome the shortcomings of the original version was considered, which was related to generating new solution vectors through eliminating the restriction of variable numbers. Moreover, the technique that evokes the violated agents into the feasible search space is improved. The steps of IRO are as follows:

Step 1: Initialization

Initialize the total number of iterations and number of light rays (LRs) randomly, including beginning point matrix and step size matrix. In what follows, the objective function (Fit) and the penalized objective function ($PFit$) are created after evaluating the initial population. Then, the light ray memory matrix (LR_M), the objective function memory (Fit_M) and penalized objective function memory ($PFit\_M$) are formed.

Step 2: Origin or cockshy point making and convergent step

Return the matrix of LRs to the starting points through eking the $stepsize$ matrix, such that if each LR existed in the search space, do it inside the search space. After that, appraise and update the new LRs, and update Fit, $PFit$, LR_M, Fit_M and $PFit\_M$. Subsequently, the normal vectors are generated. These ones begin from the origin point and terminate in the existing position of LRs. In what follows, the $stepsize$ for each LR is generated and modified, which will be utilized in the next iteration.

Step 3: Stopping criteria

For this purpose, there are two possible alternatives, including the maximum number of iterations and the maximum number of objective function evaluations. In the current research, the first one is considered as the stopping criterion.

3.2. Colliding Bodies Optimization (CBO) Algorithm

Kaveh and Mahdavi (2014) proposed CBO as a new population based meta-heuristic algorithm, which was inspired by the physics laws concerning energy and momentum that govern the collisions accrued among solid bodies. The concept of this algorithm is simple, and there are not inner parameters that the values of them can affect the performance of CBO. Initially, a set of candidate solutions are generated randomly within the search space namely the number of colliding bodies (CBs), so the matrix of CBs are formed by these objects. In what follows, Fit and $PFit$ are created after evaluating the initial objects. The mass with larger values for the candidate solutions and less $PFit$ is suitable for minimization problems, so the mass matrix of the objects is created.

These objects are classified into two groups, including stationary and moving in order to perform the collision process, such that the better ones are considered as the stationary group of objects. For this purpose, they are sorted in a rising order based on their $PFit$. Indeed, the first moiety is selected as the stationary objects, and before collision process their velocity will be zero. The remnant of them will constitute the moving objects. Also, in order to perform the collision process, they will proceed toward the equivalent stationary objects, so their velocity before this process is calculated. In what follows, after the collision process, the new velocities of them are calculated. Hence, after collision process, the new velocities are

considered as the *stepsize* for two aforementioned objects. It should be noted that the stopping criterion of CBO is the maximum number of objective function evaluations.

3.3. Solution representation

One of the crucial considerations of rendering a meta-heuristic algorithm is to decide how to characterize the solution in order to search the solution space (Mohammadi et al., 2014; Niakan et al., 2015; Vahdani et al. 2018a,b; Abad et al., 2018). For this purpose, two main solution schemes are presented including the following sections, although the other ones can be structured based on the concept of these solution schemes. The first one is concerned with the location decision of chipping terminal, which is demonstrated by a $(\mathbf{2} \times \boldsymbol{S})$ matrix, in which $\mathbf{2}$ signifies the number of rows and $\boldsymbol{S}$ denotes the number of potential chipping terminals. The first row is filled with random numbers that belong to [0,1], such that the first maximum q numbers are considered as located chipping terminals (**Fig. 3**). The second row is filled with random integer numbers that belong to $[1, L]$. For instance, Two of five chipping terminals should be located, which are the first and fourth chipping terminals, and their capacities are the second and first levels. Similarly, this structure is utilized for the location decisions of multi-modal terminals and biorefineries.

Chipping terminals				
1	2	3	4	5
0.94	0.45	0.02	0.67	0.11
⇩	$q = 2$		⇩	
1	0	0	1	0
2	1	3	1	2

Fig. 3. Chipping terminal location

The second one is concerned with the transported biomass of type $f \in F \setminus \{f_1\}$ between supplier $i \in I \setminus \{i_1\}$ and chipping terminals, which is demonstrated by a $(\boldsymbol{I} \times \boldsymbol{S})$ matrix, in which $\boldsymbol{I}$ signifies the number of suppliers $i \in I \setminus \{i_1\}$ and $\boldsymbol{S}$ denotes the number of located chipping terminals. In **Fig. 4** suppliers 1 and 4 supply the feedstock of located chipping terminal 1; suppliers 2, 5 and 6 supply the feedstock of located chipping terminal 4, and supplier 3 supplies the feedstock of located chipping terminal 3. Also, the amount of feedstock between each of them is specified. Similarly, this structure is utilized for the other supply decisions among facilities.

Biomass of type $f \in F \setminus \{f_1\}$		**Chipping Terminals**				
		1	**2**	**3**	**4**	**5**
		1	0	0	1	1
Suppliers	1	81	27	95	79	67
	2	90	54	48	95	75
	3	12	95	80	65	74
	4	91	96	14	03	39
	5	63	15	42	84	65
	6	9	97	91	93	17

Fig. 4. Amount of biomass between supplier and chipping terminal

4. Computational results

4.1. Numerical results

Several numerical examples are investigated in this section to illustrate the proposed model's accuracy and validity and meta-heuristic algorithms. The proposed model is coded in GAMS software and solved with BARON solver, and the employed meta-heuristic algorithms are coded in C++ software. Also, the specification of instances, especially the values of the model's key parameters, which is provided in Table 2, is adapted from Quddus et al. (2018). Additionally, the obtained results by GAMS and meta-heuristic algorithms are presented in Tables 3-5, which are related to the small, medium, and large size instances, respectively. It is worth noting that these results are based on the CVaR formulation of the proposed model, and a maximum CPU time of 15000 seconds is considered for GAMS's solution. Furthermore, the gap percentages of the optimality and CPU time are presented in Appendix D.

Table 2. The values of input parameters

Parameters	Values	Parameters	Values
w_{lj}, w_{lj}, w_{ls}	~uniform $(7,32) M		
$p_{f_1 i}, p_{fi}$	~uniform $(25,35) dry ton	$\bar{\Delta}_{jk}$	~uniform (0.6,0.7)
u_{jk}	~uniform $(4,6)/ton	π_g	$5/gallon
$c_{kg}, c_{fis}, c_{f_1 ik}, c_{fsk}, c_{fsjk}, c_{f_1 ijk}$	~uniform $(1,2)	φ_f	~uniform (70,75) gallons/dt
$s_{f_1 i}, s_{fi}$	~uniform $(0.7,3)/M ton	h_k	~uniform (0.28,0.34)/gallons
B	~uniform $(5,10) M	μ_g	~uniform (2,20) MG
l_k	~uniform (15,22)	σ_g^2	~uniform (1,2) MG

Table 3. Computational results on 10 small instances

Problem No.	Structure $\|I\|/\|J\|/\|S\|/\|K\|/\|G\|/\|L\|/\|F\|/\|R\|$	GAMS (BARON solver)		IRO		CBO	
		Objective function value	CPU time (Second)	Objective function value	CPU time (Second)	Objective function value	CPU time (Second)
P1	**6/6/6/6/10/3/3/3**	1,889,410	56.43	1,889,410	33.18	1,889,410	25.05
P2	**8/8/8/8/15/3/3/2**	2,477,100	74.12	2,477,100	39.05	2,477,100	33.18
P3	**10/10/10/10/15/3/3/3**	3,371,982	99.07	3,371,982	46.22	3,371,982	40.24
P4	**12/12/12/12/15/4/3/3**	3,714,563	125.61	3,714,563	50.11	3,714,563	47.63
P5	**14/14/14/14/18/3/3/4**	4,661,750	147.08	4,661,750	55.08	4,661,750	51.76
P6	**16/16/16/16/20/4/3/4**	5,955,200	169.44	5,955,200	61.14	5,955,200	58.41
P7	**18/18/18/18/22/4/3/2**	6,818,679	214.99	6,818,679	64.17	6,818,679	55.17
P8	**20/20/20/20/25/3/3/3**	7,031,681	251.57	7,031,681	70.44	7,031,681	63.39
P9	**24/24/24/24/28/3/3/3**	7,167,088	295.22	7,167,088	77.63	7,167,088	70.67
P10	**25/25/25/25/30/4/3/4**	7,297,406	387.65	7,297,406	81.31	7,297,406	68.24

Table 4. Computational results on 10 medium instances

Problem No.	Structure $\|I\|/\|J\|/\|S\|/\|K\|/\|G\|/\|L\|/\|F\|/\|R\|$	GAMS (BARON solver)		IRO		CBO	
		Objective function value	CPU time (Second)	Objective function value	CPU time (Second)	Objective function value	CPU time (Second)
P11	**30/30/30/30/40/4/3/4**	8,054,133	481.03	8,511,608	95.15	8,585,706	71.45

P12	**35/35/35/35/45/4/3/4**	8,607,110	598.10	9,138,169	106.13	9,312,893	79.23
P13	**40/40/40/40/45/4/3/3**	9,912,155	1344.41	10,686,294	100.61	10,649,619	88.04
P14	**45/45/45/45/55/4/3/2**	10,031,808	1641.30	10,941,191	115.46	10,976,303	85.46
P15	**50/50/50/50/60/4/3/4**	11,513,844	2813.66	12,931,198	117.86	13,143,053	93.61
P16	**55/55/55/55/65/3/3/3**	12,266,159	4105.35	14,180,906	122.51	14,436,145	97.45
P17	**60/60/60/60/75/4/3/4**	13,981,741	6710.72	16,227,209	111.90	15,957,361	109.98
P18	**65/65/65/65/80/3/3/4**	14,557,189	10031.45	17,311,409	136.38	17,470,083	116.55
P19	**70/70/70/70/85/4/3/4**	15,203,470	12355.98	17,987,225	127.81	17,043,090	109.51
P20	**75/75/75/75/95/3/3/3**	16,814,964	14782.69	20,250,261	148.53	20,078,749	127.37

Table 5. Computational results on 10 large instances

Problem No.	**Structure** $\|I\|/\|J\|/\|S\|/\|K\|/\|G\|/\|L\|/\|F\|/\|R\|$	**GAMS (BARON solver)**		**IRO**		**CBO**	
		Objective function value	**CPU time (Second)**	**Objective function value**	**CPU time (Second)**	**Objective function value**	**CPU time (Second)**
P21	**95/95/95/95/110/4/3/4**	-	15000	20,225,573	187.42	21,803,168	156.31
P22	**110/110/110/110/125/4/3/4**	-	15000	26,316,696	202.13	32,132,686	174.06
P23	**125/125/125/125/140/3/3/3**	-	15000	31,987,540	197.47	36,510,578	189.27
P24	**140/140/140/140/170/3/3/3**	-	15000	66,828,811	218.04	76,462,184	200.02
P25	**155/155/155/155/185/4/3/5**	-	15000	45,435,718	251.67	48,343,604	227.56
P26	**170/170/170/170/200/4/3/3**	-	15000	52,685,314	280.26	57,827,401	219.65
P27	**185/185/185/185/210/4/3/4**	-	15000	58,395,835	347.99	69,257,460	246.21
P28	**200/200/200/200/225/4/3/4**	-	15000	63,076,436	412.75	65,959,660	276.43
P29	**215/215/215/215/230/4/3/4**	-	15000	67,810,413	534.83	88,967,262	295.75
P30	**250/250/250/250/250/4/3/5**	-	15000	83,220,113	632.61	87,888,761	311.31

The results reveal no difference among the objective function values, which was obtained by GAMS and meta-heuristic algorithms for the small size instances, although these algorithms both run much faster than GAMS in all instances. In the medium-size cases, GAMS required much more CPU times than these algorithms, also in this circumstance, IRO performs slightly better than CBO in terms of objective function values, although CBO runs faster than IRO. Furthermore, in terms of objective function value, there is a gap between the employed algorithms and GAMS. These gaps range from 5.68% to 20.43% and 6.60% to 20.0.1 in IRO and CBO, respectively. What is more, while GAMS cannot solve large size instances in a reasonable time, the necessitated CPU times of IRO are more than the ones required in CBO, although IRO offers better solutions in whole cases compared to CBO. In what follows, in an attempt to specify whether there are statistically significant differences amongst performances of GAMS, IRO, and CBO, the ANOVA method is utilized, such that the obtained results are presented in Appendix E. The computational results reveal that at a 95% confidence level, there are no significant differences amongst the means of objective function values for small and medium test problems, which were obtained by GAMS and two solution methods (P-values=0.833, 0.489>0.05). This investigation is conducted to compare GAMS and two solution methods with regard to CPU times. The computational results reveal that at a 95% confidence level, there are significant differences amongst the means of CPU times for small and medium-size instances, which have been obtained by GAMS and two solution methods (P-value=0.010<0.05), while there is no significant difference between IRO and CBO for large size instances (P-value=0.077>0.05). In order to provide further investigation, Fisher's least significant difference method is utilized, where the obtained results are presented in Appendix E. Moreover, the interval plots are depicted and given in Appendix E to better show the comparisons of means of objective function values and CPU times.

4.2. Sensitivity analyses

In an attempt to illustrate the validity and correctness of the proposed model's behavior concerning changing parameters, a broad range of sensitivity analyses is provided in this section. They are included conversion rate, risk level, the comparison risk-averse and risk-neutral models, supply feedstock.

4.2.1. Conversion rate

In this section, the influence of the conversion rate on the investigated SC is demonstrated. As shown in Table 2, this rate is considered moderately low for biomass to convert to biofuel. This conversion rate could be enhanced by considering improved processes, ranging from the acquisition novel of catalyst to anaerobic digestion; new technology can also facilitate this improvement. Therefore, this is a persuading circumstance to examine the influence of the conversion rate on the investigated biomass-to-biofuel SC performance. For this purpose, the behavior of the SC is examined concerning changing biomass-to-biofuel conversion rate, such that two managerial factors, including SC costs and production level, are considered for this concern. It is worth noting, the improvements in conversion rate could realize without any further charge. As can be seen in Figs 5 and 6, at the higher amount of this rate, the SC costs for producing the identical amount of biofuel would be smaller, now that fewer biomasses would be utilized and carried. Also, the biofuel production increases by 20.88%, and the SC cost declines by 9.32% for a 20% improvement in this rate, so improving this conversion rate can be a crucial factor in managing biomass-to-biofuel SC. In this situation, the capacities of bio-refineries are regulated and administrated to minimize the total transportation costs since, in slight biomass variations, two bio-refineries with capacities of 130 and 90 MG are employed. Nevertheless, increasing the variation leads to a change in bio-refineries' capacities to 100, 70, and 50 MG. The total production capacities for bio-refineries were not changed by these variations, although the capacities are regulated to various areas for different suppliers to minimize transportation costs.

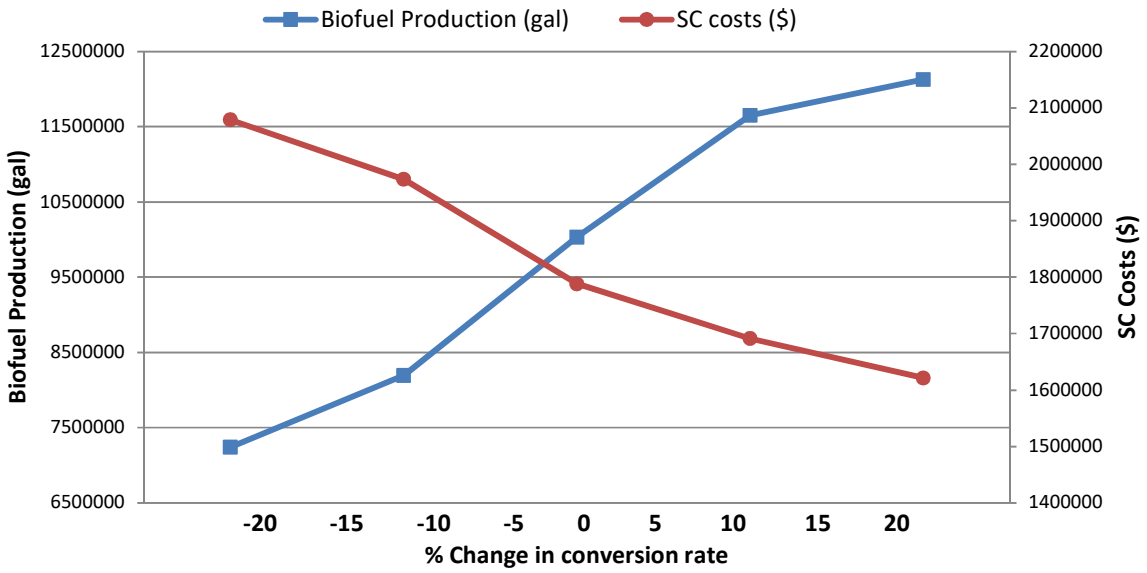

Fig 5. The influence of conversion rate on biofuel production and SC costs

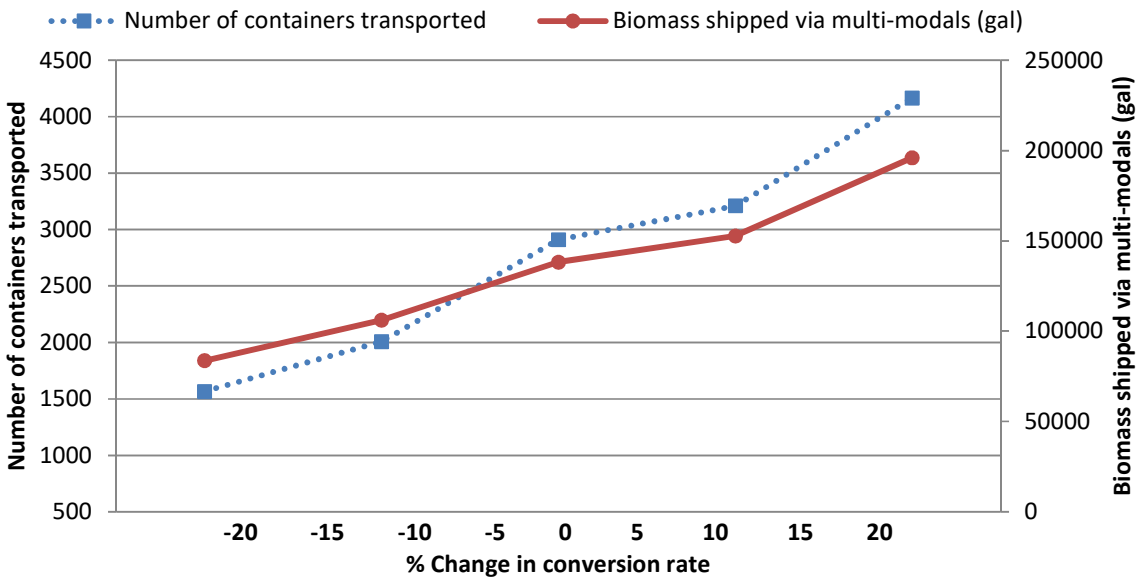

Fig 6. The influence of conversion rate on number of containers and shipping biomass

4.2.2. Risk level and attitude

In this subsection, a number of comparative analyses are conducted in order to illustrate the behavior of the proposed model under risk-neutral and risk-averse attitudes. As a consequence of the similarity between CVaR and ASD, the investigations have been made on the CVaR model without any generality loss. For this purpose, the probability of failure of the biorefinery is assumed $q_k \in [0.01,0.05]$ and risk level α takes value in {0.5,0.7,0.9,0.95} for CVaR. The obtained results are provided in Table 6 and Figs 7 to 9. As can be seen, the SC costs increase once the problem size rises, such that this trend is more intense for the risk-averse model. Indeed, this circumstance is predictable, now that DMs with risk-averse attitudes prefer to more reliable biorefinery to serve customers, although it might lead to rising transportation costs. It is worth noting that the failure cost is in contrast to SC cost. Indeed, these attitudes' comparisons reveal that the percentage of declined disruption costs is continually higher than the percentage of increased transportation costs. Therefore, a trade-off between these factors would be made by DMs according to their risk-averse attitudes. Consequently, for the higher amount of α, the proportion of declined disruption costs and increased transportation costs rises, signifying that the risk-averse model's obtained solution is more reliable than the neutral one. Moreover, the proposed model increases by 20.87% in the total SC costs under random disruptions than the risk-neutral model. This is because of opening three new facilities, and allocating some customers to more distant but more reliable bio-refineries, so transportation costs are augmented, although the failure costs of SC decline by 80.45%.

Table 6. Comparative analyses on different risk attitude ($\alpha = 0.9$)

Problem. No.	Structure $\|I\|/\|J\|/\|S\|/\|K\|/\|G\|/\|L\|/\|F\|/\|R\|$	Risk-averse attitude	Risk-neutral attitude
P1	**10/10/10/10/15/3/3/3**	3,371,982	2,911,369
P2	**50/50/50/50/60/4/3/4**	11,513,844	9,884,082
P3	**110/110/110/110/125/4/3/4**	26,316,696	21,761,138
P4	**155/155/155/155/185/4/3/5**	45,435,718	37,413,841
P5	**200/200/200/200/225/4/3/4**	63,076,436	49,935,427
P6	**250/250/250/250/250/4/3/5**	83,220,113	62,365,653

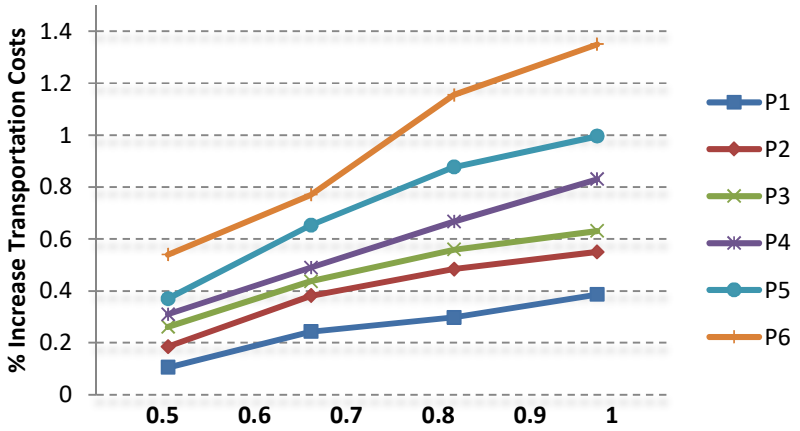

Fig 7. The percentage of increased transportation costs comparing to risk-neutral model

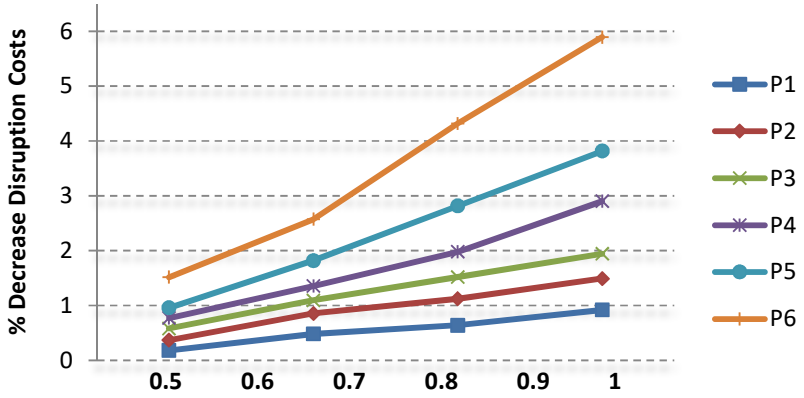

Fig 8. The percentage of decreased disruption costs comparing to risk-neutral model

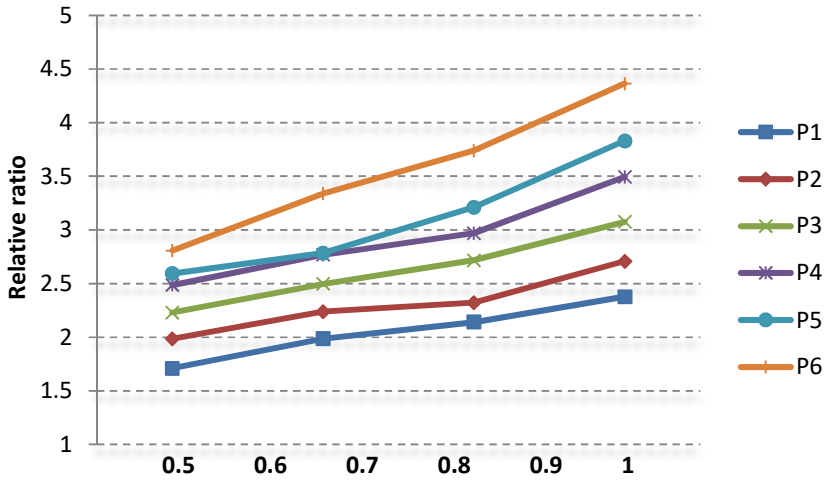

Fig 9. Relative ratio of decreased disruption costs and enlarged transportation costs

4.2.3. Feedstock supply

In order to illustrate the effect of supply feedstock on different decisions of the biomass-to-biofuel SC, a number of examinations are provided in this section. The concerned decisions are related to the number of multi-modal terminals, the unit cost of biofuel, the number of utilized containers between multi-modal terminals and biorefineries, and biofuel production. The obtained results are shown in Table 7. As can be seen, a 5% increase in feedstock supply declines the unit cost of biofuel by 14.81% ($/gallon) due to the better capacity distribution of bio-refineries as discussed in the sensitivity analysis of conversion rate. Similarly, this reduction is almost 23.64% due to a 15% increase in feedstock supply. Additionally, the number of containers and multi-modal terminals are affected by these changes, such that the numbers of multi-modal terminals approximately increase by 29% due to a 15% increase in feedstock supply with the intention of transporting these feedstocks, which results in a further 7.52% increase in the utilized containers, so the amount of biofuel production has also been affected.

Table 7. The influence of feedstock supply on biomass-to-biofuel SC

Items	Feedstock changes				
	-15%	-5%	0%	5%	15%
Unit cost of biofuel ($/gallon)	6.02	5.35	4.78	4.07	3.65
Number of multi-modal terminals	9	12	14	16	18
Number of utilized containers	67,442	75,461	78,769	82,785	90,740
Produced Biofuel (MG)	502.45	562.18	586.83	616.75	676.02

5. Conclusions

In this study, a novel mathematical model for designing a biomass-to-biofuel supply chain network was proposed in which multi-modal terminals and biorefineries as the two major facilities and the connecting link between them could be disrupted. To gain resilience and reliable framework and surmount the repercussions of the disruptions, risk-averse optimization, transitional probabilities, and spatial statistics models were employed. Since the demand for investigated SC faces uncertainty and SC encounters seasonality of raw materials, risk pooling and M/M/1 queuing system were considered to tackle these challenges. Finally, since the proposed model is an NP-hard problem, two new meta-heuristic algorithms called improved ray optimization and colliding bodies optimization were employed to solve the proposed model. The Obtained

results unfold that by increasing 20% of the conversion rate of biomass to biofuel, biofuel production increases by 20.88%, and the SC cost declines by 9.32%. Although the proposed model increases by 20.87% in the total SC costs, it decreases by 80.45% in the failure costs of SC. What is more, a 5% increase in feedstock supply declines the unit cost of biofuel by 14.81% ($/gallon) due to the better capacity distribution of bio-refineries. To extend this study, there are two main topics, including considering districting regions and service sharing within these regions to mitigate total costs, enhance the SC's efficiency, and reflect vehicle routing considerations among facilities to provide a better plan for transporting decisions.

Nomenclature

Sets and indices

I_C: Set of corn-stover suppliers
I_W: Set of forest residues suppliers
I_M: Set of MSW suppliers
I: Set of entire biomass supply resources, i.e., $I = I_C \cup I_W \cup I_M$
F: Set of biomass types (f_1 for corn-stover, f_2 for forest residues and f_3 for MSW)
J: Set of multi-modal terminals
S: Set of chipping terminals
K: Set of biorefineries
G: Set of customers
L: Set of capacities
E: Emergency biorefinery
R: Backup level for customers $0 \leq R \leq |k|$

Parameters

w_{lj}: Opening cost for a multi-modal terminal with capacity l at location j
w_{lk}: Opening cost for a biorefinery with capacity l at location k
w_{ls}: Opening cost for a chipping terminal with capacity l at location s
$p_{f_1 i}$: Unit cost of procurement for the biomass of type f_1 at location $i \in I \setminus \{i_2, i_3\}$
p_{fi}: Unit cost of procurement for the biomass of type $f \in F \setminus \{f_1\}$ at location $i \in I \setminus \{i_1\}$
u_{jk}: Fixed cost of container for transporting biomass from multi-modal terminal j to biorefinery k
c_{kg}: Unit transportation cost of biofuel from biorefinery k to customer g
c_{fis}: Unit transportation cost for the biomass of type $f \in F \setminus \{f_1\}$ from supplier $i \in I \setminus \{i_1\}$ to chipping terminal $s \in S$
$c_{f_1 ik}$: Unit transportation cost for the biomass of type f_1 from supplier $i \in I \setminus \{i_2, i_3\}$ to biorefinery k
c_{fsk}: Unit transportation cost for the biomass of type $f \in F \setminus \{f_1\}$ from chipping terminal s to biorefinery k
c_{fsjk}: Unit transportation cost for the biomass of type $f \in F \setminus \{f_1\}$ from chipping terminal s through multi-modal terminal j to biorefinery k
$c_{f_1 ijk}$: Unit transportation cost for the biomass of type f_1 from supplier $i \in I \setminus \{i_2, i_3\}$ through multi-modal terminal j to biorefinery k
e_{fs}: Unit cost of chipping for biomass $f \in F \setminus \{f_1\}$ at chipping terminal s
cp_{lk}: Unit cost of production of bio-fuel at biorefinery k with capacity l
$s_{f_1 i}$: Available amount of biomass of type $f_1$at supplier $i \in I \setminus \{i_2, i_3\}$
s_{fi}: Available amount of biomass of type $f \in F \setminus \{f_1\}$ at supplier $i \in I \setminus \{i_1\}$
cap_{jk}: Capacity to transport biomass containers from multi-modal terminal j to biorefinery k
ca_{ls}: Biomass storage capacity at chipping terminal s with capacity l

ca_{lj}: Biomass storage capacity at multi-modal terminal j with capacity l
ca_{lk}: Biomass storage capacity at biorefinery k with capacity l
$pca_{l\,k}$: Biofuel production capacity at biorefinery k with capacity l
B: Total available budget for fortification
$\bar{\Delta}_{jk}$: Maximum reliability that could be obtained for arc (j,k)
r_{jk}: Cost related to the mitigation of reliability for arc (j,k)
π_g: Unit compensation cost of unfulfilled demand for customer g
φ_f: Rate of conversion (tons/gallons) from biomass of type $f \in F$ to bio-fuel
r_f: Rate of conversion (tons/ tons) to chip biomass of type $f \in F \setminus \{f_1\}$
q_j: Probability of failure of multi-modal terminal j
q_k: Probability of failure of biorefinery k
q_{jk}: Probability of failure of arc (j,k)
f_k: Fixed inventory ordering cost at biorefinery k
h_k: Per unit per year inventory holding cost at biorefinery k
μ_g: Mean customer demand g
σ_g^2: Variance of customer demand g
l_k: Order lead time from biorefinery k
$\mathcal{C}_0$: Congestion cost
α: Service/ Risk level
z_α: Standard normal deviate
β, θ: Weight coefficients allocated to transportation and inventory costs of biofuel, respectively

Decision variables

x_{fis}: Amount of biomass of type $f \in F \setminus \{f_1\}$ transported from supplier $i \in I \setminus \{i_1\}$ to chipping terminal s
x_{f_1ik}: Amount of biomass of type f_1 transported from supplier $i \in I \setminus \{i_2, i_3\}$ to biorefinery k
x_{fsk}: Amount of biomass of type $f \in F \setminus \{f_1\}$ transported from chipping terminal s to biorefinery k
x_{fsjk}: Amount of biomass of type $f \in F \setminus \{f_1\}$ transported from chipping terminal s through multi-modal terminal j to biorefinery k
x_{f_1ijk}: Amount of biomass of type f_1 transported from supplier $i \in I \setminus \{i_2, i_3\}$ through multi-modal terminal j to biorefinery k
z_{jk}: Number of containers utilized to transport biomass from multi-modal terminal j to biorefinery k
p_{lk}: Amount of biofuel produced at biorefinery k with capacity l
Δ_{jk}: Reliability improvement gained by fortifying arc (j,k)
y_{ls}: 1 if a chipping terminal with capacity l is opened in location s; 0 otherwise
y_{lj}: 1 if a multi-modal terminal with capacity l is opened in location j; 0 otherwise
y_{lk}: 1 if a biorefinery with capacity l is opened in location k; 0 otherwise
z_{gkr}: 1 if biorefinery k is assigned to customer g at level r; 0 otherwise
p_{gkr}: Probability that biorefinery k is assigned to customer g at level r

Supply chain (SC)
Improved ray optimization (IRO)
Colliding bodies optimization (CBO)
Resilient supply chain (RSC)
Municipal solid waste (MSW)
Absolute-semi deviation (ASD)

Conditional value at risk (CVaR)
Decision makers (DMs)
Value-at-risk (VaR)
Colliding bodies (CBs)
Objective function (Fit)
Penalized objective function ($PFit$)
Light ray memory matrix (LR_M),
Objective function memory (Fit_M)
Penalized objective function memory ($PFit\_M$)

Appendix A. Linearization of Eq. (10).

To linearize the congestion term, let a new decision variable $V = \{V_k\}_{k\in K}$ as follows.

$$V_k = \frac{\sum_{i\in I_c} x_{f_1 ik} + \sum_{f\in F\setminus\{f_1\}}\sum_{s\in S} x_{fsk} + \sum_{f\in F\setminus\{f_1\}}\sum_{s\in S}\sum_{j\in J} x_{fsjk} + \sum_{i\in I_c}\sum_{j\in J} x_{f_1 ijk}}{\sum_{l\in \text{£}} ca_{lk} y_{lk} - \left(\sum_{i\in I_c} x_{f_1 ik} + \sum_{f\in F\setminus\{f_1\}}\sum_{s\in S} x_{fsk} + \sum_{f\in F\setminus\{f_1\}}\sum_{s\in S}\sum_{j\in J} x_{fsjk} + \sum_{i\in I_c}\sum_{j\in J} x_{f_1 ijk}\right)}$$

So this equation can be written as follows:

$$\sum_{i\in I_c} x_{f_1 ik} + \sum_{f\in F\setminus\{f_1\}}\sum_{s\in S} x_{fsk} + \sum_{f\in F\setminus\{f_1\}}\sum_{s\in S}\sum_{j\in J} x_{fsjk} + \sum_{i\in I_c}\sum_{j\in J} x_{f_1 ijk} = \left(\frac{V_k}{1+V_k}\right)\sum_{l\in L} ca_{lk} y_{lk} = \sum_{l\in L} ca_{lk}\left(\frac{V_k}{1+V_k}\right) y_{lk}$$

Now another continuous variable $A = \{A_{lk}\}_{l\in L, k\in K}$ is defined as follows:

$$A_{lk} = \left(\frac{V_k}{1+V_k}\right) y_{lk} \qquad \forall l \in L, \forall k \in K$$

Once $\sum_{l\epsilon L} y_{lk} = 1$, we have:

$$\sum_{l\epsilon L} A_{lk} = \frac{V_k}{1+V_k} \qquad \forall k \in K$$

when $y_{lk} = 0$, this equation compels $A_{lk} = 0$, which is compelled by utilizing further constraints $0 \le A_{lk} \le y_{lk}$ $\forall l \in L, \forall k \in K$.

Appendix B. Proof of Eqs. (18)-(20).

In order to provide CVaR-based risk-averse model, let $X = \left(x_{fis} \cup x_{f_1 ik} \cup x_{fsk} \cup x_{fsjk} \cup x_{f_1 ijk}\right)$, $\Delta = \left(\Delta_{jk}\right)$, $Z = \left(z_{jk} \cup z_{gkr}\right)$, $P = \left(p_{lk} \cup p_{gkr}\right)$ and $Y = \left(y_{ls} \cup y_{lj} \cup y_{lk}\right)$ signify the solutions of the proposed model, and a particular set $\mathcal{Z}$ is defined that

$$\mathcal{Z} = \{(X, Y, Z, P, \Delta): \text{Constraints}\}$$

Such that it signifies the feasible region common to the whole of proposed model, in what follows, we are concerned to control the risk of transportation costs for each customer g. With respect to the definition of CVaR, the metrics for risks of uncertain costs for customer g subject to risk level α are as follows (Yu et al., 2017):

$$\varphi_g(P, Z) = \min_{\eta_g\in\mathbb{R}}\left\{\eta_g + (1-\alpha)^{-1}\sum_{k\in K}\sum_{r=0}^{R} p_{gkr}\left(z_{gkr}\beta\mu_g c_{kg} - \eta_g\right)_+\right\}$$

This problem can be reformulated as $\min_{(X,Y,Z,P,\Delta)\in\mathcal{Z}}\{\mathcal{R}: \varphi_g(P,Z) \le \psi_g, \forall g \in G\}$, where the inward constraints impel the risk value for each customer lower a predefined level ψ_g for all $g \in G$. In order to linearize CVaR model, a linearization method is applied, which was proposed by Krokhmal et al., (2002) and Uryasev (2000). Let $\mathcal{M}_{gkr}$ substitute the nonlinear terms $\left(z_{gkr}\mu_g\beta c_{kg} - \eta_g\right)_+$ and adding Eqs. (19) and (20) (Yu et al., 2017). In what follows, by describing $\eta = (\eta_g)$ and $\mathcal{M} = (\mathcal{M}_{gkr})$, Eq. (18) can be obtained.

Appendix C. Proof of Eqs. (21)-(23).

In order to provide CVaR-based risk-averse model, regarding to Eq. (14), the risk of transportation costs for each customer g in terms of ASD with risk level λ is as follows (Yu et al., 2017):

$$\chi_g(P,Z) = \inf_{\eta_g\in\mathbb{R}} \sup_{\kappa\in[0,1]} \left\{ \sum_{k\in K}\sum_{r=0}^{R} p_{gkr}\left[z_{gkr}\mu_g\beta c_{kg} + \lambda\kappa\left(\eta_g - z_{gkr}\mu_g\beta c_{kg}\right) + \lambda\left(z_{gkr}\mu_g\beta c_{kg} - \eta_g\right)\right]\right\}$$

Hence, the risk-averse optimization problem in terms of ASD is as follows:

$$\min_{(X,Y,Z,P,\Delta)\in\mathcal{Z}} \left\{ \mathcal{R} + \sum_{g\in G} \chi_g(P,Z) \right\}$$

This problem can be reformulated as:

$$\min_{(X,Y,Z,P,\Delta)\in\mathcal{Z}} \{\mathcal{R}: \chi_g(P,Z) \le \psi_g, \forall g \in G\}$$

By utilizing the aforementioned linearization method, we have:

$$\chi_g(P,Z) = \inf_{\eta_g\in\mathbb{R}} \sup_{\kappa\in[0,1]} \left\{ \sum_{k\in K}\sum_{r=0}^{R} p_{gkr}\left[z_{gkr}\mu_g\beta c_{kg} + \lambda\kappa\left(\eta_g - z_{gkr}\mu_g\beta c_{kg}\right) + \lambda\mathcal{M}_{gkr}\right]\right\}$$

$$= \inf_{\eta_g\in\mathbb{R}} \max\left\{ \sum_{k\in K}\sum_{r=0}^{R} p_{gkr}\left[z_{gkr}\mu_g\beta c_{kg} + \lambda\mathcal{M}_{gkr}\right], \sum_{k\in K}\sum_{r=0}^{R} p_{gkr}\left[z_{gkr}\mu_g\beta c_{kg} + \lambda\left(\eta_g - z_{gkr}\mu_g\beta c_{kg}\right) + \lambda\mathcal{M}_{gkr}\right]\right\}$$

In order to primary ASD model, let $\mathcal{F}_g$ substitute the max operator and adding Eqs. (22) and (23) (Yu et al., 2017). In what follows, by describing $\mathcal{F} = (\mathcal{F}_g)$, Eq. (21) can be obtained.

Appendix D. Gap results

Table D1. Optimality and CPU time gap percentages for ten small instances

Problem No.	Structure $\lvert I\rvert/\lvert J\rvert/\lvert S\rvert/\lvert K\rvert/\lvert G\rvert/\lvert L\rvert/\lvert F\rvert/\lvert R\rvert$	$Gap_{IRO(Objective)} = \left(\frac{IRO-GAMS}{GAMS}\right)\times 100$	$Gap_{CBO(Objective)} = \left(\frac{CBO-GAMS}{GAMS}\right)\times 100$	$Gap_{CBO-IRO(Objective)} = \left(\frac{CBO-IRO}{IRO}\right)\times 100$	$Gap_{GAMS(CPU)} = \left(\frac{GAMS-CBO}{CBO}\right)\times 100$	$Gap_{IRO(CPU)} = \left(\frac{IRO-CBO}{CBO}\right)\times 100$
P1	6/6/6/6/10/3/3/3	0.0	0.0	0.0	125.27	32.46
P2	8/8/8/8/15/3/3/2	0.0	0.0	0.0	123.39	17.69
P3	10/10/10/10/15/3/3/3	0.0	0.0	0.0	146.20	14.86
P4	12/12/12/12/15/4/3/3	0.0	0.0	0.0	163.72	5.21
P5	14/14/14/14/18/3/3/4	0.0	0.0	0.0	184.16	6.41
P6	16/16/16/16/20/4/3/4	0.0	0.0	0.0	190.09	4.67
P7	18/18/18/18/22/4/3/2	0.0	0.0	0.0	289.69	16.31

P8	**20/20/20/20/25/3/3/3**	0.0	0.0	0.0	296.86	11.12
P9	**24/24/24/24/28/3/3/3**	0.0	0.0	0.0	317.74	9.85
P10	**25/25/25/25/30/4/3/4**	0.0	0.0	0.0	468.07	19.15

Table D2. Optimality and CPU time gap percentages for ten medium instances

Problem No.	Structure $\lvert I\rvert/\lvert J\rvert/\lvert S\rvert/\lvert K\rvert/\lvert G\rvert/\lvert L\rvert/\lvert F\rvert/\lvert R\rvert$	$Gap_{IRO(Objective)} = \left(\frac{IRO - GAMS}{GAMS}\right) \times 100$	$Gap_{CBO(Objective)} = \left(\frac{CBO - GAMS}{GAMS}\right) \times 100$	$Gap_{CBO-IRO(Objective)} = \left(\frac{CBO - IRO}{IRO}\right) \times 100$	$Gap_{GAMS(CPU)} = \left(\frac{GAMS - CBO}{CBO}\right) \times 100$	$Gap_{IRO(CPU)} = \left(\frac{IRO - CBO}{CBO}\right) \times 100$
P11	**30/30/30/30/40/4/3/4**	5.68	6.60	0.87	573.24	33.17
P12	**35/35/35/35/45/4/3/4**	6.17	8.20	1.91	654.89	33.95
P13	**40/40/40/40/45/4/3/3**	7.81	7.44	-0.34	1427.04	14.28
P14	**45/45/45/45/55/4/3/2**	9.06	9.42	0.32	1820.55	35.10
P15	**50/50/50/50/60/4/3/4**	12.31	14.15	1.64	2905.73	25.91
P16	**55/55/55/55/65/3/3/3**	15.61	17.69	1.80	4112.78	25.72
P17	**60/60/60/60/75/4/3/4**	16.06	14.13	-1.66	6001.76	1.75
P18	**65/65/65/65/80/3/3/4**	18.92	20.01	0.92	8506.99	17.01
P19	**70/70/70/70/85/4/3/4**	18.31	12.10	-5.25	11182.97	16.71
P20	**75/75/75/75/95/3/3/3**	20.43	19.41	-0.85	11506.10	16.61

Table D3. Optimality and CPU time gap percentages for ten large instances

Problem No.	Structure $\lvert I\rvert/\lvert J\rvert/\lvert S\rvert/\lvert K\rvert/\lvert G\rvert/\lvert L\rvert/\lvert F\rvert/\lvert R\rvert$	$Gap_{CBO-IRO(Objective)} = \left(\frac{CBO - IRO}{IRO}\right) \times 100$	$Gap_{IRO(CPU)} = \left(\frac{IRO - CBO}{CBO}\right) \times 100$
P21	**95/95/95/95/110/4/3/4**	7.80	19.90
P22	**110/110/110/110/125/4/3/4**	22.10	16.13
P23	**125/125/125/125/140/3/3/3**	14.14	4.33
P24	**140/140/140/140/170/3/3/3**	14.41	9.01
P25	**155/155/155/155/185/4/3/5**	6.40	10.60
P26	**170/170/170/170/200/4/3/3**	9.76	27.59
P27	**185/185/185/185/210/4/3/4**	18.60	41.34
P28	**200/200/200/200/225/4/3/4**	4.57	49.31
P29	**215/215/215/215/230/4/3/4**	31.20	80.84
P30	**250/250/250/250/250/4/3/5**	5.61	103.21

Appendix E. Statistical results

The results of ANOVA, Fisher's test and interval plots are provided in this section.

Table E1. ANOVA computational results for small and medium cases with regard to the objective function

Source	DF	SS	MS	F	P-Value
Algorithms	2	9.60215E+12	4.80108E+12	0.18	0.833
Error	57	1.49065E+15	2.61518E+13		
Total	59	1.50026E+15			

Table E2. ANOVA computational results for large cases with regard to the objective function

Source	DF	SS	MS	F	P-Value
Algorithms	1	2.39227E+14	2.39227E+14	0.5	0.489
Error	18	8.63484E+15	4.79713E+14		
Total	19	8.87406E+15			

vTable E3. ANOVA computational results for small and medium instances with regard to CPU time

Source	DF	SS	MS	F	P-Value
Algorithms	2	101052830	50526415	7.45	0.001
Error	57	386528674	6781205		
Total	59	487581504			

Table E4. ANOVA computational results for large instances with regard to CPU time

Source	DF	SS	MS	F	P-Value
Algorithms	1	46909	46909	3.51	0.077
Error	18	240549	13364		
Total	19	287458			

Table E5. Fisher 95% individual confidence intervals in small and medium instances in terms of the CPU time

Algorithms	Lower	Upper	Significant difference at 95% level
GAMS & IRO	-4395	-1097	Yes
GAMS & CBO	-4409	-1111	Yes
IRO & CBO	-1662	1636	No

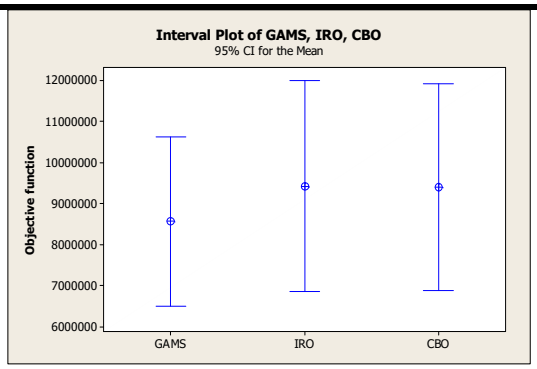

Interval plot of the objective function for small and medium instances

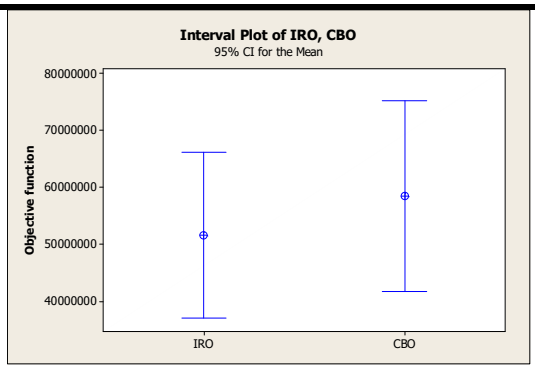

Interval plot of the objective function for large instances

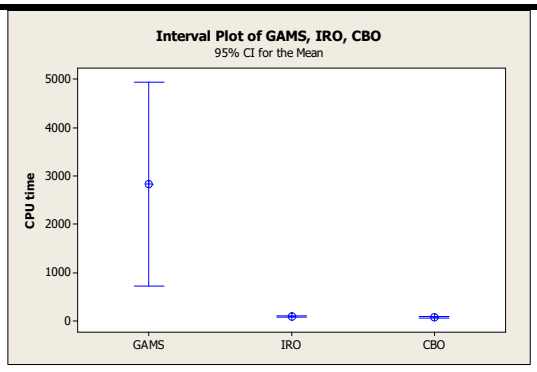

Interval plot of the CPU time for small and medium instances

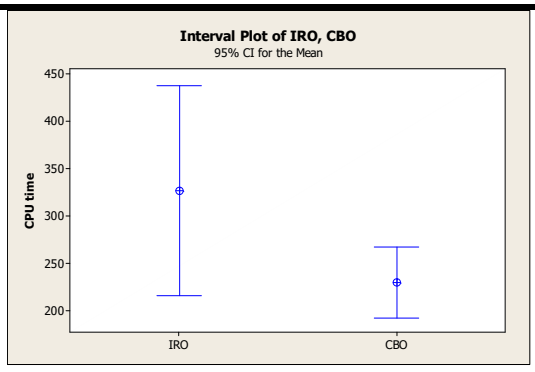

Interval plot of the CPU time for large instances

Fig E1. Interval plots of the objective function values and CPU times

References

Artzner, P., Delbaen, F., Eber, J.M. and Heath, D., 1999. Coherent measures of risk. Mathematical finance, 9(3), pp.203-228.

Abad, H.K.E., Vahdani, B., Sharifi, M. and Etebari, F., 2018. A bi-objective model for pickup and delivery pollution-routing problem with integration and consolidation shipments in cross-docking system. Journal of Cleaner Production, 193, pp.784-801.

Cui, T., Ouyang, Y. and Shen, Z.J.M., 2010. Reliable facility location design under the risk of disruptions. Operations research, 58(4-part-1), pp.998-1011.

Daskin, M.S., Coullard, C.R. and Shen, Z.J.M., 2002. An inventory-location model: Formulation, solution algorithm and computational results. Annals of operations research, 110(1-4), pp.83-106.

Elluru, S., Gupta, H., Kaur, H. and Singh, S.P., 2019. Proactive and reactive models for disaster resilient supply chain. Annals of Operations Research, 283(1-2), pp.199-224.

Elhedhli, S. and Wu, H., 2010. A Lagrangean heuristic for hub-and-spoke system design with capacity selection and congestion. INFORMS Journal on Computing, 22(2), pp.282-296.

Fattahi, M., Govindan, K. and Keyvanshokooh, E., 2017. Responsive and resilient supply chain network design under operational and disruption risks with delivery lead-time sensitive customers. Transportation research part E: Logistics and transportation review, 101, pp.176-200.

Gong, J., Mitchell, J.E., Krishnamurthy, A. and Wallace, W.A., 2014. An interdependent layered network model for a resilient supply chain. Omega, 46, pp.104-116.

Hasani, A., Mokhtari, H. and Fattahi, M., 2020. A multi-objective optimization approach for green and resilient supply chain network design: A real-life Case Study. Journal of Cleaner Production, p.123199.

Ji, L., Zheng, Z., Wu, T., Xie, Y., Liu, Z., Huang, G. and Niu, D., 2020. Synergetic optimization management of crop-biomass coproduction with food-energy-water nexus under uncertainties. Journal of Cleaner Production, 258, p.120645.

Jin, E., Mendis, G.P. and Sutherland, J.W., 2019. Integrated sustainability assessment for a bioenergy system: A system dynamics model of switchgrass for cellulosic ethanol production in the US midwest. Journal of Cleaner Production, 234, pp.503-520.

Kaveh, A. and Khayatazad, M., 2012. A new meta-heuristic method: ray optimization. Computers & structures, 112, pp.283-294.

Kaveh, A., Ghazaan, M.I. and Bakhshpoori, T., 2013. An improved ray optimization algorithm for design of truss structures. Periodica Polytechnica Civil Engineering, 57(2), pp.97-112.

Kaveh, A. and Mahdavi, V.R., 2014. Colliding bodies optimization: a novel meta-heuristic method. Computers & Structures, 139, pp.18-27.

Lim, C.H., How, B.S., Ng, W.P.Q. and Lam, H.L., 2019. Debottlenecking of biomass element deficiency in a multiperiod supply chain system via element targeting approach. Journal of Cleaner Production, 230, pp.751-766.

Markowitz, H.M. and Todd, G.P., 2000. Mean-variance analysis in portfolio choice and capital markets (Vol. 66). John Wiley & Sons.

Marufuzzaman, M., Eksioglu, S.D., Li, X. and Wang, J., 2014. Analyzing the impact of intermodal-related risk to the design and management of biofuel supply chain. Transportation Research Part E: Logistics and Transportation Review, 69, pp.122-145.

Margolis, J.T., Sullivan, K.M., Mason, S.J. and Magagnotti, M., 2018. A multi-objective optimization model for designing resilient supply chain networks. International Journal of Production Economics, 204, pp.174-185.

Mohammadi, S., Darestani, S.A., Vahdani, B. and Alinezhad, A., 2020. A robust neutrosophic fuzzy-based approach to integrate reliable facility location and routing decisions for disaster relief under fairness and aftershocks concerns. Computers & Industrial Engineering, 148, p.106734.

Mohammadi, M., Dehbari, S. and Vahdani, B., 2014. Design of a bi-objective reliable healthcare network with finite capacity queue under service covering uncertainty. Transportation Research Part E: Logistics and Transportation Review, 72, pp.15-41.

Momenikiyai, M., Ebrahimnejad, S. and Vahdani, B., 2018. A bi-objective mathematical model for inventory distribution-routing problem under risk pooling effect: robust meta-heuristics approach. Economic Computation & Economic Cybernetics Studies & Research, 52(4).

Niakan, F., Vahdani, B. and Mohammadi, M., 2015. A multi-objective optimization model for hub network design under uncertainty: An inexact rough-interval fuzzy approach. Engineering Optimization, 47(12), pp.1670-1688.

Ngan, S.L., How, B.S., Teng, S.Y., Leong, W.D., Loy, A.C.M., Yatim, P., Promentilla, M.A.B. and Lam, H.L., 2020. A hybrid approach to prioritize risk mitigation strategies for biomass polygeneration systems. Renewable and Sustainable Energy Reviews, 121, p.109679.

Poudel, S., Marufuzzaman, M., Quddus, M., Chowdhury, S., Bian, L. and Smith, B., 2018. Designing a reliable and congested multi-modal facility location problem for biofuel supply chain network. Energies, 11(7), p.1682.

Poudel, S.R., Marufuzzaman, M. and Bian, L., 2016. Designing a reliable bio-fuel supply chain network considering link failure probabilities. Computers & Industrial Engineering, 91, pp.85-99.

Pavlov, A., Ivanov, D., Pavlov, D. and Slinko, A., 2019. Optimization of network redundancy and contingency planning in sustainable and resilient supply chain resource management under conditions of structural dynamics. Annals of Operations Research, pp.1-30.

Quddus, M.A., Chowdhury, S., Marufuzzaman, M., Yu, F. and Bian, L., 2018. A two-stage chance-constrained stochastic programming model for a bio-fuel supply chain network. International Journal of Production Economics, 195, pp.27-44.

Rezapour, S., Farahani, R.Z. and Pourakbar, M., 2017. Resilient supply chain network design under competition: A case study. European Journal of Operational Research, 259(3), pp.1017-1035.

Rockafellar, R.T. and Uryasev, S., 2000. Optimization of conditional value-at-risk. Journal of risk, 2, pp.21-42.

Rockafellar, R.T. and Uryasev, S., 2002. Conditional value-at-risk for general loss distributions. Journal of banking & finance, 26(7), pp.1443-1471.

Quddus, M.A., Chowdhury, S., Marufuzzaman, M., Yu, F. and Bian, L., 2018. A two-stage chance-constrained stochastic programming model for a bio-fuel supply chain network. International Journal of Production Economics, 195, pp.27-44.

Salimi, F. and Vahdani, B., 2018. Designing a bio-fuel network considering links reliability and risk-pooling effect in bio-refineries. Reliability Engineering & System Safety, 174, pp.96-107.

Shapiro, A., 2013. On Kusuoka representation of law invariant risk measures. Mathematics of Operations Research, 38(1), pp.142-152.

Snyder, L.V. and Daskin, M.S., 2005. Reliability models for facility location: the expected failure cost case. Transportation Science, 39(3), pp.400-416.

Tolooie, A., Maity, M. and Sinha, A.K., 2020. A two-stage stochastic mixed-integer program for reliable supply chain network design under uncertain disruptions and demand. Computers & Industrial Engineering, p.106722.

Ulucak, R., 2020. Linking biomass energy and CO2 emissions in China using dynamic Autoregressive-Distributed Lag simulations. Journal of Cleaner Production, 250, p.119533.

Vahdani, B., Veysmoradi, D., Shekari, N. and Mousavi, S.M., 2018a. Multi-objective, multi-period location-routing model to distribute relief after earthquake by considering emergency roadway repair. Neural Computing and Applications, 30(3), pp.835-854.

Vahdani, B., Veysmoradi, D., Noori, F. and Mansour, F., 2018b. Two-stage multi-objective location-routing-inventory model for humanitarian logistics network design under uncertainty. International journal of disaster risk reduction, 27, pp.290-306.

Vahdani, B., Niaki, S.T.A. and Aslanzade, S., 2017. Production-inventory-routing coordination with capacity and time window constraints for perishable products: Heuristic and meta-heuristic algorithms. Journal of Cleaner Production, 161, pp.598-618.

Vahdani, B., Tavakkoli-Moghaddam, R., Modarres, M. and Baboli, A., 2012. Reliable design of a forward/reverse logistics network under uncertainty: a robust-M/M/c queuing model. Transportation Research Part E: Logistics and Transportation Review, 48(6), pp.1152-1168.

Wang, L., Zhao, N. and Liu, D., 2020. Complex disaster management: A dynamic game among the government, enterprises, and residents. Journal of Cleaner Production, p.122091.

Zahiri, B., Zhuang, J. and Mohammadi, M., 2017. Toward an integrated sustainable-resilient supply chain: A pharmaceutical case study. Transportation Research Part E: Logistics and Transportation Review, 103, pp.109-142.

Yildiz, H., Yoon, J., Talluri, S. and Ho, W., 2016. Reliable supply chain network design. Decision Sciences, 47(4), pp.661-698.

Yu, G., Haskell, W.B. and Liu, Y., 2017. Resilient facility location against the risk of disruptions. Transportation research part B: methodological, 104, pp.82-105.

Yu, L., Li, Y.P., Shan, B.G., Huang, G.H. and Xu, L.P., 2018. A scenario-based interval-stochastic basic-possibilistic programming method for planning sustainable energy system under uncertainty: a case study of Beijing, China. Journal of cleaner production, 197, pp.1454-1471.

Zahraee, S.M., Golroudbary, S.R., Shiwakoti, N., Kraslawski, A. and Stasinopoulos, P., 2019. An investigation of the environmental sustainability of palm biomass supply chains via dynamic simulation modeling: A case of Malaysia. Journal of Cleaner Production, 237, p.117740.

Zhu, S. and Fukushima, M., 2009. Worst-case conditional value-at-risk with application to robust portfolio management. Operations research, 57(5), pp.1155-1168.

Zhu, B., Wen, B., Ji, S. and Qiu, R., 2020. Coordinating a dual-channel supply chain with conditional value-at-risk under uncertainties of yield and demand. Computers & Industrial Engineering, 139, p.106181.

Zhang, F., Johnson, D.M. and Wang, J., 2016. Integrating multimodal transport into forest-delivered biofuel supply chain design. Renewable energy, 93, pp.58-67.

Graphical abstract: